INFORMATION TO USERS

This material was produced from a microfilm copy of the original document. While the most advanced technological means to photograph and reproduce this document have been used, the quality is heavily dependent upon the quality of the original submitted.

The following explanation of techniques is provided to help you understand markings or patterns which may appear on this reproduction.

1. The sign or "target" for pages apparently lacking from the document photographed is "Missing Page(s)". If it was possible to obtain the missing page(s) or section, they are spliced into the film along with adjacent pages. This may have necessitated cutting thru an image and duplicating adjacent pages to insure you complete continuity.

2. When an image on the film is obliterated with a large round black mark, it is an indication that the photographer suspected that the copy may have moved during exposure and thus cause a blurred image. You will find a good image of the page in the adjacent frame.

3. When a map, drawing or chart, etc., was part of the material being photographed the photographer followed a definite method in "sectioning" the material. It is customary to begin photoing at the upper left hand corner of a large sheet and to continue photoing from left to right in equal sections with a small overlap. If necessary, sectioning is continued again — beginning below the first row and continuing on until complete.

4. The majority of users indicate that the textual content is of greatest value, however, a somewhat higher quality reproduction could be made from "photographs" if essential to the understanding of the dissertation. Silver prints of "photographs" may be ordered at additional charge by writing the Order Department, giving the catalog number, title, author and specific pages you wish reproduced.

5. PLEASE NOTE: Some pages may have indistinct print. Filmed as received.

Xerox University Microfilms
300 North Zeeb Road
Ann Arbor, Michigan 48106

Neutron Absorption Cross Sections of Radioactive Nuclides

by

Robert S. Rundberg

A dissertation submitted to the Graduate Faculty in Chemistry in partial fulfillment of the requirements for the degree of Doctor of Philosophy, The City University of New York.

1978

This manuscript has been read and accepted for the Graduate Faculty in Chemistry in satisfaction of the dissertation requirement for the degree of Doctor of Philosophy.

4/28/78
date

Chairman of Examining Committee

4/28/78
date

Executive Officer

David C. Lorke

Evan T Williams

Supervisory Committee

The City University of New York

Synopsis.

Absorption cross sections, resonance integrals and neutron temperatures of reactor produced radioactive nuclides were measured in the Brookhaven High Flux Beam Reactor and the Brookhaven Medical Research Reactor. The effective absorption cross sections in general depend on many parameters these being variable from reactor to reactor and also in different positions in a given reactor. These parameters are, epithermal index (this depends on the degree of moderation and the moderating medium) , neutron temperature(very dependent on moderator), resonance integral, Westcott g, and to a lesser degree target temperature. The aim of the research described here is to determine as many of these parameters as possible for various radionuclides after activation in a reactor. The first part of this work describes a method in which a radionuclide is both created and burned up, which yields cross section data for the adsorption process. This method is used to screen nuclides of interest for nuclides having large adsorption cross sections which affect reactors most profoundly. The method is applied to various target materials. A method is then developed for determining more specific data about the cross section from reactor measurments, that is the Breit

Wigner parameters for a single level resonance. This method can only be applied to cross sections displaying a neutron temperature dependence. The particular case of ^{22}Na was studied; the existence of a temperature dependence in the thermal cross section was determined and the Breit Wigner parameters estimated based on reactor data measured in two different reactors. In addition the effect of doppler broadening on the cross sections of light nuclides is examined and calculated using the Debye model.

Acknowledgements

The author wishes to express deepest gratitude to the members of his thesis committee for their advice and suggestions in preparing this thesis, with special thanks to Prof. Harmon L. Finston and Prof. Evan T. Williams whose sometimes forceful encouragement made this thesis posssible.

The author also wishes to thank:
J.J. Floyd and Dave Rorer of Brookhaven National Labs for their assistance in using the HFBR,
Ottmar Safferling for his excellent workmanship and teaching the author the rudiments of glassblowing,
Armand Gazes for his help in using the Data Acquisition center,
Lucia M. Babcock, Dr. Sene Bauman, and Allen Rychtman for making it all more pleasant.

It is the author's wish to dedicate this thesis to his parents.

List of tables

List of Figures

TABLE OF CONTENTS

I. Introduction

Accurate measurements of neutron cross sections are important to both nuclear technology and theory in order to design efficient nuclear power reactors. Resonances in neutron cross sections, which correspond to a high cross section over a well defined narrow energy interval, characterize the energy levels of highly excited nuclei, i.e. ,compound nuclei, and are therefore useful for nuclear structure studies.

A dramatic demonstration of the technical and economic impact of a large neutron cross section is a consequence of the discovery of a huge resonance in plutonium-240 at 1.056 eV (ref. 1). The neutron-spectroscopy group at Columbia University, in 1947, discovered a strong resonance at approximately 1 eV with a peak cross section of about 200,000 barns, and a width of about 30 milli-eV. At this time all information about plutonium was classified and this interesting information remained unavailable. The DuPont engineers, contracted in 1951 to design new plutonium production facilities, carefully examined the operating characteristics of the Hanford reactors and observed a decrease in reactivity with time, which could not be accounted for by

any absorption process then known. The excess reactivity of the Savannah River reactor was therefore increased to permit operation for a longer period between fuel changes, but this required an elaborate control-rod mechanism. Fortunately the design engineers learned of the Columbia data and with this information were able to simplify the control rod mechanism design saving millions of dollars.

The ratio of cross section for neutron capture to that for fission, α, or alpha(ref. 2), is particularly important in breeder reactors. Thus accurate cross-section measurements are especially important for fissile materials. The ratio is necessary to calculate the breeding gain, G,

$$G = \frac{\text{number } ^{239}\text{Pu produced}}{\text{number } ^{239}\text{Pu consumed}} - 1$$

the number ratio of ^{239}Pu atoms produced to those consumed, minus 1. This is of economic and technical importance to the design of both breeder reactors and light water reactors since alpha is necessary in the calculation of neutron efficiency, in the calculation of the reactor fuel inventory, and the calculation of the flux distribution across the reactor. Fuel can be utilized more efficiently in light water reactors by converting ^{238}U to ^{239}Pu.

The cross sections of nonfissionable materials are also important to reactor design, since nuclides arising from the fission process can influence the operation of a reactor. Neutron capture by such high neutron capture cross

section fission products as ^{135}Xe(ref. 3), ^{147}Pm(ref. 4), ^{148m}Pm(ref. 5), and ^{148}Nd(ref. 6) reduce the the overall reactivity. The transient behavior of a reactor, particularly at shutdown, depends on the properties of such fission products as ^{135}Xe, ^{105}Rh, ^{149}Sm, and ^{151}Sm(ref. 7). Reactor poisons such as ^{135}Xe, due to the decay of ^{135}I, can prevent the restart of a reactor after shutdown for at least 48 hours if the fuel elements are not replaced.

Gamma rays from fission products are used to monitor the burnup of fuel, i.e., the increase in fission product activity corresponds to the depletion of fissile fuel. Therefore the reliability of this monitoring depends, inter alia, on the accurate knowledge of fission product capture cross sections.

The cross section for ^{22}Na is obviously of particular importance to sodium cooled fast breeder reactors, because ^{22}Na can be produced by the $^{23}Na(n,2n)^{22}Na$ reaction. If the coolant is exposed to a sufficient fast neutron flux there will be significant production of ^{22}Na, and since this nuclide has a very large cross section, an accurate measurement is necessary. It proved difficult to measure the cross section of this nuclide accurately, because, as we have discovered and will describe in detail, it is temperature dependent owing to a resonance in the thermal region. A method for determining cross sections of such nuclides is

developed.

The resonance in ^{22}Na is also of particular interest because there is little detailed information about the levels associated with neutron capture to the ^{23}Na compound nucleus, and there is the same lack of information about the levels in the isobaric analogue state of magnesium.

Methods for determining neutron cross sections.

The principle means of determining cross sections are time-of-flight spectrometry, neutron activation, and burnup. The latter two methods will yield only measurements of thermal neutron cross sections and resonance integrals. The burnup technique is essentially the same as neutron activation; activation applies to the cross section for neutron capture by a stable nuclide resulting in the production of radioactivity while burnup applies to the depletion of a radioactive nuclide by neutron capture.

The excitation function for neutron induced reactions is best determined via a time-of-flight spectrometer. This method uses short pulses of an intense neutron beam which travel along a flight path (often quite long, e.g. 300 meters) to achieve resolution of neutron energy, the fastest neutrons arriving at the target first. The reaction is monitored by multichannel scaling so that a profile of the reac-

tion vs. time (1 over velocity) results. The rate of reaction is observed via an appropriate nuclear spectroscopic technique. A two parameter spectrum, such as γ-γ or γ-β coincidence, can be measured so that the cross section to different nuclear states can be determined.

The source of neutrons can be an accelerator which produces neutrons by a charged particle induced reaction, or a neutron reactor equipped with a chopper (to produce a pulsed neutron beam), or a pulsed reactor. Accelerators are most useful for resonance studies at high and intermediate energies, and high flux reactors at low energies (near thermal and cold neutrons). The total cross section is usually determined by a transmission experiment, and most of the available excitation functions are for total cross sections of stable nuclides, as measured with a neutron detector of some sort.

There have been few determinations of total cross sections of radioactive nuclides. In addition to the problems normally associated with time-of-flight spectrometry, there are several additional serious problems presented by radioactive nuclides. It is often difficult or very expensive to manufacture a sufficiently thick target to get a measureable change in the intensity of transmitted neutrons. A number of problems arise with handling of large quantities of radioactive materials ,such as shielding, and unless

there are no gamma rays emitted by the nuclide of interest, there will be a large increase in the background, which can interfere with the measurement of radiative capture.

A notable example of this type of measurement was that of Stokes et al. who used 360 Ci of ^{182}Ta.

Bibliography

1. J.L. Fowler and W.W. Havens Jr., Physics Today, 29, #8, August, p. 42 (1976).

2. A.M. Weinberg and E.P. Wigner, "The Physical theory of Neutron Chain Reactors", University of Chicago Press.

3. H.R. Fickel and R.H. Tomlinson, Can. J. Phys., 37, 531(1959).

4. D.R. Bidinosti, H.R. Fickel and R.H. Tomlinson, Second Geneva Conf., Vol. 15, p.459.

5. R.P. Schuman and J.R. Berreth, Nuclear Sci. Eng., 12, 519(1962).

6. C.P. Ruiz, J.P. Peterson Jr. and B.F. Rider, Trans. Am. Nuclear Soc., 7, 270(1964).

7. A.M. Weinberg, E.P. Wigner, "The Physical Theory of Neutron Chain Reactors", p.600, University of Chicago Press.

8. Loren C. Schmid, "Critical Assemblies and Reactor Research", Wiley-Interscience, New York(1971), p.330.

9. "Experimental Neutron Resonance Spectroscopy", J.A. Harvey Ed. Academic Press(1970).

10. G.E. Stokes, J.R. Berreth, R.P. Schuman, O.D. Simpson, and T.E. Young, Trans. Am. Nuclear Soc., 6, 41(1963).

Theory

Nuclear models of neutron nucleus interactions.

Bethe, Fermi and others, (ref 1) first attempted to explain neutron-nucleus interactions using quantum mechanics in 1935. They assumed that the potential between the neutron and the nucleus had the form of a spherical square well. This, with some refinements, is usually called the optical model because the results, when the model is applied to neutron scattering, resemble the dispersion of light as it passes through a refracting medium. Resonances are predicted by the theory, but they are widely spaced, broad and dominated by scattering. Experiments by Szilard, Fermi and others (ref 2) proved conclusively that neutron resonances at low energy are predominantly due to radiative capture, are extremely narrow, and are closely spaced. Nevertheless the optical model is useful at intermediate neutron energies and the model predicts a 1/v cross section at low energies, a prominent feature of neutron capture cross sections.

Niels Bohr, (ref 3) in 1936, proposed the compound nucleus to explain the observed resonances at low neutron energy. Bohr pointed out that since the observed widths of the resonances were on the order of 1 eV, the Heisenberg un-

certainty gives a half-life of the nucleus, after absorbing a neutron, of about 10^{-15} sec. This is about 1000 times longer than the time expected for a 100 eV neutron to traverse the nucleus. This indicates the formation of an intermediate state which exists long enough to distribute the energy of the system over the entire nucleus, and for the excited nucleus to "forget" how it was formed. Thus the excited nucleus will decay through some process (called an exit channel) independent of its mode of formation.

These two basic models form the foundation for the calculation and interpretation of neutron absorption cross sections. These models are presented in more detail starting with the optical model which is presented for its historical and conceptual significance rather than for any practical application to effective neutron cross sections.

The optical model.

Both the scattering and absorption of neutrons can be described by the optical model (ref. 4,5), with the scattering of intermediate energy neutrons likened to the scattering of light by a sphere of non-absorbing but refracting material. The neutron wave is refracted by the nuclear potential of the nucleus just as a light wave is refracted in going through a crystal ball. The simple optical model is one in which the nuclear interaction is represented

by a real potential well.

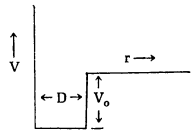

$$V = V(r) \quad \text{for } r<D$$
$$V = 0 \quad \text{for } r>D \tag{II.1}$$

This model is applicable only to elastic neutron scattering. The formalism can be extended to describe processes such as absorption and inelastic scattering which proceed through a compound nucleus, by replacing the real potential with a complex one. This extended model is called "the cloudy crystal ball" model, and has the potential

$$V(r) = -(V_o + iW) \tag{II.2}$$

The introduction of the imaginary potential causes the amplitude of the scattered wave to be less than the incident wave. If the potential is complex, then the wave number must also be complex. The wave number can be written

$$k = \left[\frac{2m}{\hbar^2}[(E + V_o) + iW] \right]^{1/2} \tag{II.3}$$

where k is,

$$k = k_r + iK_i \tag{II.4}$$

Expanding k as a Taylor series around W=0 enables the following first order approximations for k_r and K_i to be made,

$$k_r = \frac{2m}{h^2}\sqrt{E + V_o} \tag{II.5}$$

$$K_i = \frac{W}{2\sqrt{h^2/2m(E+V_o)}} \tag{II.6}$$

and the wave function is

$$\phi = \exp(\pm ikx) \tag{II.7}$$

The probability of finding a particle between x and x+dx becomes

$$|\phi|^2 = [\exp(-ikr)\exp(-K_i x)][\exp(ik_r x)\exp(-K_{ix})] = \exp(-2K_i x) \tag{II.8}$$

Thus the probability diminishes exponentially and is characterized by the mean free path, Λ, (which is defined as the distance at which the probability becomes 1/e)

$$\frac{1}{\Lambda} = 2K_i = \frac{N_a \sigma}{A} \tag{II.9}$$

The mean free path can also be expressed in terms of the

density of nucleons within the nucleus, ρ, and the effective average cross section, σ, for the interaction of the incident particle with the nucleons within the nucleus. Thus the cross section is proportional to K_i which can be equal to the imaginary part of the complex quantity k.

$$\sigma = \frac{K_i A}{\rho N_a}\left(\frac{\hbar^2}{2m}(E + V_o)\right)^{1/2} \qquad \text{(II.10)}$$

The optical model is not able to predict the various possible reactions that may occur at medium energies nor the resonances that are observed in slow neutron reactions. These phenomena are consistent with the compound nucleus model. Nevertheless, an approximation of the mean free path using experimentally derived data will show that it is much larger than nuclear dimensions thus lending credence to the basic hypothesis of the compound nucleus which envisions a captured particle being trapped within a complex system for a comparatively long time; thus its energy can be distributed throughout the ensemble of nucleons, so that the identity of the incident nucleon is lost.

The compound nucleus.

Niels Bohr (ref. 6) first emphasized the compound-nucleus model for nuclear reactions. He assumed that when some target nucleus, A, is bombarded by an incident particle, a, the two may coalesce to form a compound nucleus

(A+a), where the parentheses indicate an intermediate state (i.e. a compound nucleus) produced at an excitation energy dictated by the energy of the bombarding particle. It is assumed that there is a strong interaction between all the nucleons in the compound nucleus including the bombarding particle and that the incident particle loses its independent identity and the total energy of the excited compound nucleus is shared by all the nucleons present. The compound nucleus also has a relatively long lifetime compared to the time required for a nucleon to cross the nucleus. The same compound nucleus may be produced by the bombardment of a different nucleus with a different incident particle, usually at a different incident energy. Thus,

$$(A+a) = (B+b) \qquad \text{(II.11)}$$

so that the properties of the compound nucleus are independent of the mode of formation.

The second step in the reaction is the relaxation of the compound nucleus which can dissociate via various exit channels. The competition for the exit channels does not depend on the way in which the compound nucleus is formed. Any reaction in which a compound nucleus is formed can be represented as follows.

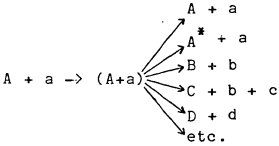

(II.12)

Cross sections for nuclear reactions often contain resonances (sharp increases in the cross section at a discrete excitation energy). The energy of a resonance corresponds to the energy of a level in the compound nucleus. The shape of a resonance is best described by the Breit-Wigner (ref. 7) formula for neutron capture

$$\sigma(n,\gamma) = \pi\lambda^2 \left[\frac{2I_c + 1}{(2I_n + 1)(2I_t + 1)} \right] \frac{\Gamma_n \Gamma_\gamma}{(E_n - E_o)^2 + (\Gamma/2)^2} \qquad \text{(II.13)}$$

where

λ = the de Broglie wavelength of the incident neutron

$I_n = 1/2$ = the spin of the bombarding neutron

I_t = the spin of the target nucleus

I_c = the angular momentum of the compound nucleus

E_n = the kinetic energy of the incident neutron

E_o = the kinetic energy of neutron which just forms level E of the compound nucleus

Γ_γ = width of excited level for γ emission

Γ_n = width of excited level for neutron emission

Γ = total width of excited level

Usually the following simplified form of the Breit-Wigner formula is used for S-wave neutrons:

$$\sigma(E_n) = \frac{\sigma_o 1/\sqrt{E_n}}{(E_n - E_o)^2 + (\Gamma/2)^2} \qquad \text{(II.14)}$$

where $\lambda\!\!\!^{-}_n$ is replaced by the de Broglie wavelength of the neutron ($1/\sqrt{E_n}$) and the remaining parameters are summarized in σ_o the maximum cross section of the resonance.

Nuclear cross sections

The probability for any nuclear reaction can be expressed in terms of cross section. This concept originates from the simple idea that the probability for the reaction between a nucleus and an impinging particle is proportional to the cross sectional area presented by the nucleus. The rate of reaction for a beam of particles striking a thin target (assuming the beam is only infinitesimally attenuated) for a particular process, is defined by the equation (ref. 8):

$$R = I(1 - e^{-n\sigma x}) \qquad \text{(II.15)}$$

where R is the number of processes occurring in the target per unit time

I is the number of incident particles per unit time

n is the number of target nuclei per cubic centimeter of target

σ is the cross section for the specified process, expressed in square centimeters

x is the target thickness in centimeters.

This equation expressed in terms of flux rather than intensity is,

$$\frac{dN}{dt} = -\sigma \phi N \qquad \text{(II.16)}$$

where

N is the number of target nuclei

ϕ is the number of incident neutrons per square centimeter second.

The above equations apply to monoenergetic beams of particles. If we apply these relations to the reaction rate of nuclei in a reactor, the energy dependence of neutron cross section and, in addition, the variation of the neutron intensity on energy must be considered.

Enrico Fermi (ref. 9) discovered, in the early days of nuclear physics, that the neutron absorption cross section of nuclei exposed to monoenegetic neutrons from a radium-beryllium source increased when the neutrons were moderated by a material such as paraffin. The 1/v dependence

(where v is the velocity of the neutron) of neutron absorption cross sections was attributed to the reaction probability being proportional to the time the neutron spends in the vicinity of the nucleus.

If we consider thermal neutrons as being in equilibrium with the moderating medium, the energy distribution will be a Maxwell-Boltzman distribution (ref. 10), thus the reaction rate can be treated as an average over the entire range of neutron energies. The thermal cross section is defined as the cross section for neutrons having a velocity of 2200 meters per second. The 1/v cross section is then,

$$\sigma(v) = \sigma_o(\frac{v_o}{v}) \qquad \text{(II.17)}$$

where

σ_o is the 2200 meter per second cross section

v_o is 2200 meters per second

v is the neutron velocity

and the flux

$$\phi = n(v) \cdot v \qquad \text{(II.18)}$$

where

n(v) is the neutron density distribution.

Therefore the reaction rate for an infinitesimal range of neutron velocities is,

$$\frac{dN}{dt} = -N\sigma_o n(v) \qquad (II.19)$$

If n(v) is a Maxwell-Boltzman distribution then,

$$n(v) = n\frac{\pi}{2}\left(\frac{2m}{\pi}kT\right) v^2 e^{\left(-\frac{mv}{2kT}\right)^2}. \qquad (II.20)$$

and the average reaction rate is,

$$R = n\frac{\pi}{2}\left(\frac{2m}{\pi}kT\right) v^2 e^{\left(-\frac{mv}{2kT}\right)^2} v\sigma_o\left(\frac{v}{v_o}\right) \qquad (II.21)$$

$$R = \sigma_o n v_o \qquad (II.22)$$

Thus, for a 1/v neutron absorber in a Maxwell-Boltzman distribution of neutron velocities the reaction rate can be expressed in terms of the cross section at a single neutron velocity and the neutron density. It is also important to note that because the velocity factor in the flux is canceled by the 1/v factor in the cross section, the temperature dependent part of the Maxwell-Boltzman distribution cancels due to normalization.

Effective neutron cross sections

The Westcott convention is a method by which one can calculate the effective reactor cross section from the 2200 meter per second cross section and the resonance integral, if these parameters are known. On the other hand

given the reactor measurements, i.e., the effective cross section and the cadmium ratio (the ratio of activities produced, simultaneously in identical samples irradiated with and without cadmium shielding), the 2200 meter per second cross section and the resonance integral can be calculated. The Westcott convention considers that the neutron spectrum of a reactor is constituted of two parts : the Maxwell-Boltzman distribution corresponding to the effective neutron temperature T, and the epithermal 1/E flux distribution, cut off at a suitable lower limit of energy. The cross section in the thermal region is first assumed to be 1/v and then is corrected for any deviation from the 1/v law. The effective cross section is composed of the sum of this thermal cross section plus any resonances above the cadmium cutoff.

The effective neutron cross section, $\hat{\sigma}$, is defined by equating the reaction rate per atom per second, R, to the product of $\hat{\sigma}$ with nv_o, the 2200 m/sec flux:

$$R = \hat{\sigma} n v_o \qquad \text{(II.23)}$$

where n is the neutron density, including both thermal and epithermal neutrons, and v_o = 2200 m/sec. The effective cross section in the Westcott convention is

$$\hat{\sigma} = \sigma_o (g+rs) \qquad \text{(II.24)}$$

where

$\hat{\sigma}$ = the effective cross section

σ_o = the thermal cross section (2200 meters/second cross section)

g = correction factor for non 1/v absorbers

r = the epithermal index

s = the contribution to the effective cross sections from epithermal resonances

It is important to note that r depends entirely on the specific irradiation conditions within the reactor.

The neutron flux as a function of energy was shown to have two separable components in a well moderated reactor (ref. 14). A 1/E component due to "slowing down" neutrons and a thermal component, which in the basic Westcott formalism is assumed to be adequately described by a Maxwell-Boltzman distribution. It has also been shown that the cutoff between the two components occurs at ~5kT for heavy water reactors. This distribution is shown in the following equation.[1]

$$n(v) = n(1 - f) \rho_m(v) + nf \rho_e(v) \qquad (II.25)$$

1. Equations II.25 through II.50 comprise the Westcott formulism and are compiled from references 11-13.

where f is the fraction of neutrons above the cutoff energy ρ_m and ρ_e are the Maxwellian and epithermal density distribution functions respectively, and ρ_m and ρ_e are normalized such that,

$$\int_0^\infty \rho_m(v)\, dv = \int_0^\infty \rho_e(v)\, dv = 1 \quad . \tag{II.26}$$

The Maxwellian component can be written

$$\rho_m(v) = \frac{4}{\sqrt{\pi}} \frac{v^2}{v_T^3} e^{-(\frac{v}{v_T})^2} \tag{II.27}$$

and the epithermal component

$$\rho_e(v) = v_T \sqrt{\mu}\ v^{-2}\ \triangle \tag{II.28}$$

where $v_T = v_o(T/T_o)^{\frac{1}{2}}$ and $\triangle = 1$ if $E>\mu kT$, $\triangle=0$ if $E<\mu kT$. Thus, the beginning of the epithermal distribution is defined by, $\triangle$, a cutoff function. If the cross section as function of neutron velocity is combined with this neutron flux, the reaction rate per atom becomes

$$R = nv_o\bar{\sigma} = \int_0^\infty n(v)\sigma(v)\cdot v dv$$

$$= n(1 - f)\int_0^\infty \frac{4}{\sqrt{\pi}} \frac{v^3}{v_T^3} e^{-(\frac{v}{v_T})^2} \sigma(v)dv$$

$$+ nf\, v_T\sqrt{\mu} \int_0^\infty \frac{\Delta}{v} \sigma(v)dv \qquad \text{(II.29)}$$

The Westcott g is defined as the ratio of the effective Maxwellian cross section to the 2200 meter per second cross section. It occurs as a correction to the effective cross section in eqn. II.24 and is defined in the following expression by averaging the actual cross section over a Maxwell-Boltzman flux

$$g = \frac{\bar{\sigma}_m}{\sigma_o} = \frac{1}{v_o\sigma_o}\int_0^\infty \frac{4}{\sqrt{\pi}} \frac{v^3}{v_T^3} e^{-(\frac{v}{v_T})^2} \sigma(v)dv. \qquad \text{(II.30)}$$

Inserting eqn. II.30 in eqn. II.29 the reaction rate per atom becomes

$$R = n(1 - f)\cdot v_o\bar{\sigma}_m + nf\cdot v_T\sqrt{\mu}\int_0^\infty \frac{\Delta}{v} \sigma(v)dv$$

$$= nv_o\bar{\sigma}_m + nf\,[\, v_T\sqrt{\mu}\int_0^\infty \frac{\Delta}{v} \sigma(v)dv - v_o\bar{\sigma}_m\,] \qquad \text{(II.31)}$$

Remembering that $v_o = \sqrt{\frac{2kT}{m}}$ the last term in eqn. II.30 can rewritten in terms of the following integral

$$v_o\bar{\sigma}_m = \bar{\sigma}_m v_T\sqrt{\mu}\int_0^\infty (v_o/v) \frac{\Delta}{v} dv \qquad \text{(II.32)}$$

by combining eqn. II.31 with eqn. II.23 the effective cross section becomes

$$\bar{\sigma} = g\sigma_o + \frac{f}{2}\frac{\mu}{}\frac{v_T}{v_o}\int_0^\infty \left[\sigma(v) - \frac{v_o\bar{\sigma}_m}{v}\right]\frac{\Delta}{E}\,dE \qquad \text{(II.33)}$$

The resonance absorption integral is defined simply as the average of the cross section over the epithermal flux. Since the epithermal flux is normalized the resonance integral, Σ, is

$$\Sigma = \int_{\mu kT}^\infty \sigma(E)\,\frac{dE}{E} \qquad \text{(II.34)}$$

The resonance integral in excess of the effective Maxwellian cross section is defined by subtracting all 1/v capture occuring in the epithermal region from the resonance integral.

$$\Sigma' = \Sigma - g\sigma_o\int_{\mu kT}^\infty \sqrt{\frac{E_o}{E}}\,\frac{dE}{E} \qquad \text{(II.35)}$$

Substituting eqn. II.34 into eqn. II.35 we get

$$\Sigma' = \int_0^\infty \left[\sigma(v) - \frac{v_o\bar{\sigma}_m}{v}\right]\frac{\Delta dE}{E} \quad . \qquad \text{(II.36)}$$

It is convenient to define the quantity, r, which replaces the epithermal fraction, f, in the above expressions

$$r = \frac{f\sqrt{\pi\mu}}{4} \quad , \qquad \text{(II.37)}$$

and since = 5, r is almost equal to f (r=1.02f). Replacing f with r the neutron density becomes

$$n(v) = \frac{4}{\sqrt{\pi}}\, n\left[\left(1 - f \right) \frac{v^2}{v_T^3} e^{-\left(\frac{v}{v_T}\right)^2} + r \cdot v_T \frac{\Delta}{v^2} \right] \qquad \text{(II.38)}$$

and the effective cross section is

$$\bar{\sigma} = g\sigma_o + \left(\frac{4T}{\pi T_o}\right)^{\frac{1}{2}} r \int_0^{\infty} \left[\sigma(v) - \sigma_m \frac{v_o}{v} \right] \frac{\Delta}{E} dE \quad . \qquad \text{(II.39)}$$

The remaining integral can now be defined as the quantity, s,

$$s = \left(4\frac{T}{\pi T_o}\right)^{\frac{1}{2}} \int_0^{\infty} \left[\sigma(v) - \sigma_m \frac{v_o}{v} \right] \frac{\Delta}{E} dE \qquad \text{(II.40)}$$

which can be shown to be proportional to the reduced resonance integral by inserting the expression eqn. II.36 into eqn. II.40 to give

$$s = \frac{1}{\sigma_o} \left(\frac{4T}{\pi T_o}\right)^{\frac{1}{2}} \Sigma' \qquad \text{(II.41)}$$

so that s may be calculated from the excitation function.

On the other hand given s and σ_o from reactor measurements, Σ' can be determined

$$\Sigma' = s\sqrt{\frac{T_o}{T}}\sigma_o \quad \frac{\sqrt{\pi}}{2} \tag{II.42}$$

The normalization factor $(\frac{4T}{\pi T_o})^{1/2}$ is carried into eqn. II.41 from the definition of ρ_e causing s to be temperature dependent. It is convenient to replace the parameter s by a temperature independent term since neutron temperature data are not usually available for various irradiation positions. Thus,

$$s_o = s\sqrt{\frac{T_o}{T}} \tag{II.43}$$

where T_o = 296.3 ^oK. Correspondingly, the quantity

$$r' = r\sqrt{\frac{T}{T_o}} \tag{II.44}$$

can be found (rather than r if the temperature is uncertain) utilizing a cadmium ratio technique.

The cadmium ratio, R_{Cd} , defined as the experimentally determined ratio of activities in samples without and with cadmium shielding, is equal to the ratio of the rates of neutron capture in the respective samples. For a pure

1/v absorber the cadmium ratio becomes

$$R_{Cd} = \frac{1}{fv_T\sqrt{\mu}\int_{E_{Cd}}^{\infty}\frac{\Delta}{v^2}dv} = \frac{1}{4\pi}\left(\frac{\#E_{Cd}}{kT}\right)^{\frac{1}{2}} \qquad (II.45)$$

and is determined only by the cadmium cutoff energy and the fraction of epithermal flux. The cadmium cutoff energy depends on the thickness of the cadmium shield (i.e. the total absorptivity) and is proportional to a factor K defined below. Generally, when there is a resonance in the cross section, the ratio is

$$R_{Cd} = \frac{(g + rs)}{\frac{r}{K}\sqrt{\frac{T}{T_o}} + rs} \qquad (II.46)$$

The denominator is the rate of neutron capture in the cadmium shielded sample. The epithermal flux is unaffected by the cadmium shield (resonance-capture rate equals rs); however, the capture rate of thermal neutrons is considerably reduced. The only capture due to the 1/v part is for the neutrons with energies greater than the cadmium cutoff. The flux of such neutrons is a function of reactor temperature and the thickness of the cadmium used. The rate of 1/v capture under the cadmium shield is given by $\sigma_o(r'/K)\ nv_o$, where K is a coefficient for a given thickness of cadmium calculated from the known variation of the cadmium cross

section with energy. Thus the rate of neutron capture under the cadmium shield is given by the denominator of eqn. II.46. Rearranging, and substituting for s from eqn. II.43, and solving for r'(= $r\sqrt{T/T_o}$) we obtain

$$r' = \frac{g}{R_{Cd}(1/K+s_o) - s_o} \qquad \text{(II.47)}$$

Values of K for various thicknesses of cadmium have been tabulated and s_o is known for ^{60}Co(ref 15a) and ^{197}Au (ref 15b). The cadmium ratio and the rate of reaction are determined experimentally for cobalt flux wires. The epithermal index (obtained via eqn. II.47) and s_o for ^{59}Co are multiplied to give rs and since g=1 for ^{59}Co (ref. 15), Eq. II.24 is solved. The flux, nv_o, is then obtained from Eq. II.23. Equation II.47 is rearranged to give

$$s_o = \frac{g-R_{Cd}r'/K}{r'(R_{Cd} - 1)} \qquad \text{(II.48)}$$

In a burnup experiment the experimental value of R_{Cd} for the nuclide under study is substituted into Eq. II.48 to give s_o for that nuclide: σ is calculated from Eq. II.23 and, assuming g=1 (that is, an absence of a thermal resonance), a value for σ_o is obtained from Eq. II.24.

The resonance integral Σ of the target nuclide is the total absorption cross section with a suitable lower en-

ergy limit and is usually defined as in eqn. II.35. It is calculated from the Westcott parameter, s , and the thermal cross section:

$$\Sigma' = s \sqrt{\frac{T_o}{T}}\, \sigma_o \frac{\pi^{1/2}}{2} \qquad \text{(II.49)}$$

and by using eqn. II.35

$$\Sigma = \Sigma' + \sigma_o \sqrt{\frac{4T_o}{T}} \qquad \text{(II.50)}$$

The treatment of resonances below the cadmium cutoff and the calculation of g will be treated seperately in a later section.

The Westcott procedure has been applied to the simultaneous production and burnup of any nuclide (ref. 16), radioactive or stable, in a reactor irradiation. For a reaction of the general form

$$X(n,q)Y(n,u)Z$$

where

X is the target nucleus

Y is the nuclide of interest

q = 2n,p,d, , etc.

u = γ,p, etc.

the rate equation is

$$\frac{dN}{dt} = \sigma_{(n,q)} M \phi_{prod} - \lambda N - \bar{\sigma} n v_o N \qquad \text{(II.51)}$$

where

$\sigma(n,q)$ is the cross section for production of Y

ϕ_{prod} is the flux for production

M is the number of target atoms of X

λ is the decay constant of Y

N is the number of atoms of Y

and $\bar{\sigma}$ is the effective cross section for burnup of Y

Since cross sections for the production of Y are typically of the order of millibarns, M may be assumed constant. Integrating from N = 0 at t=0 to N=N at t=t

$$N_1 = M \frac{\sigma(n,q)\phi_{prod}[1 - \exp-(\lambda + \bar{\sigma} n v_o)t\ ]}{\lambda + \bar{\sigma} n v_o} \qquad \text{(II.52)}$$

Assuming that the transmission of fast neutrons through the cadmium is 100%, the ratio of activity in the cadmium-shielded sample to that of the bare sample immediately following irradiation is given by

$$R_{Cd} = \frac{N_1^{Cd}}{N_1^{bare}} = \frac{[1 - \exp-(\lambda + \bar{\sigma}^{Cd} n v_o)t\ ]\ (\lambda + \bar{\sigma} n v_o)}{[1 - \exp-(\lambda + \bar{\sigma} n v_o)t\ ]\ (\lambda + \bar{\sigma}^{Cd} n v_o)} \qquad \text{(II.53)}$$

where

$$\sigma^{Cd} = \sigma_o \left(g \frac{\sqrt{\frac{T}{T_o}}}{K} + rs \right) \qquad \text{(II.54)}$$

Note that although R^1_{Cd} is the ratio of activity in the cadmium-wrapped sample to the bare sample, it does not correspond to cadmium ratio as defined in eqn. II.46. In addition, also note that $rs = r\sqrt{\frac{T}{T_o}} s \sqrt{\frac{T_o}{T}}$.

This one equation is not sufficient to give us both the thermal cross section and s_o. Both these parameters can be determined by irradiating the original sample a second time in a reactor position where r is sufficiently different to give another independent equation. This is achieved by irradiating first near the core (in a position where the Westcott convention applies) where the rate of production is adequate to determine the initial activity ratio R^1_{Cd}. The samples are then reirradiated at a second reactor position sufficiently far from the core so that production of Y is negligible or at least significantly reduced and a second activity ratio, R^2_{Cd}, is determined. The increased distance from the core results in greater moderation of the neutron flux which lowers the epithermal index. Under these conditions, the following differential equation can be written:

$$\frac{dN}{dT} = -\lambda N - \bar{\sigma} nv_o N \qquad \text{(II.55)}$$

This equation is essentially the same as Eq. 2.2.28 with the production term omitted (assuming that the production reaction has no thermal component). Note, however that $r\sqrt{\frac{T}{T_o}}$ and nv_o will be different for each irradiation position.

Integrating from $N=N_1$ at $t=0$ to $N=N_2$ at $t=t$ (duration of the second irradiation) we obtain {note that the measured N_1 will be less than N_1 previously defined in Eq. II.51 due to decay}

$$N_2 = N_1 e^{-(\lambda + \bar{\sigma} nv_o)t} \qquad \text{(II.56)}$$

The ratio, R^2_{Cd}, is the measured ratio of activity of Y in the cadmium-wrapped sample to that of the bare sample, and is given by

$$R^2_{Cd} = R^1_{Cd} \frac{e^{-(\lambda + \bar{\sigma}_{Cd} nv_o)t}}{e^{-(\lambda + \bar{\sigma} nv_o)t}} \qquad \text{(II.57)}$$

$$= e^{(\bar{\sigma} - \bar{\sigma}_{Cd}) nv_o t} \qquad \text{(II.58)}$$

$$= e^{-[\sigma_o (\, g - \frac{r\sqrt{\frac{T}{T_o}}}{K}) nv_o t]} \qquad \text{(II.59)}$$

Taking the natural log and rearranging, we obtain:

$$\ln(R_{Cd}^2/R_{Cd}^1) = \sigma_o\left(g - \frac{r\sqrt{\frac{T}{T_o}}}{K}\right)nv_o t \qquad \text{(II.60)}$$

$$\sigma_o = \frac{\ln(R_{Cd}^2/R_{Cd}^1)}{\left(g - r\sqrt{\frac{T}{T_o}}\right)nv_o t} \qquad \text{(II.61)}$$

In Eqs. II.54 through II.60, σ, nv_o, rs, and r refer to the second irradiation position and g is again assumed to be unity. If we are able to employ a reactor position far enough away from the core so that r /K is negligible (Maxwell-Boltzman distribution only), then eqn. II.60 assumes the following simple form:

$$\sigma_o = \frac{\ln(R_{Cd}^2/R_{Cd}^1)}{gnv_o t} \qquad \text{(II.62)}$$

Doppler broadening of nuclear cross sections

The width of resonances in neutron cross sections are of the order of thermal energies so that the effect of target motion can not be neglected. The cross section for a nuclear reaction depends on the relative energy of the interacting system, not simply on the velocity of the neutron in the laboratory reference frame. The effective cross section for a given neutron velocity is defined as (ref. 17),

$$v_n\,\bar{\sigma}(v_n) = \int_{-\infty}^{\infty} |v_n - V_T|\,\sigma(|v_n - V_T|)\,P(V_T)dV_T \qquad \text{(II.63)}$$

where

v_n is the neutron velocity (laboratory reference frame)

V_T is the target atom velocity

$\tilde{\sigma}$ is the effective cross section

σ the cross section

P is the the probabilty distribution for the target atoms

If one applies this to the simple case when the cross section is 1/v,

$$\sigma(|v_n - V_T|) = \frac{c}{|v_n - V_T|} \tag{II.64}$$

inserting eqn. II.63 into eqn. II.62 and since P is normalized the effective cross section becomes,

$$\tilde{\sigma}(v_n) = \frac{c}{v_n} \int P(V_T)dV_T = \frac{c}{v_n} = \sigma(v_n) \tag{II.65}$$

Thus for a 1/v cross section there is no Doppler broadening.

The Doppler broadening can easily be calculated for a free gas; although target materials are normally solid the free gas velocity distribution can be assumed by using the Debye model or the Einstein model for solid crystals. Treating the target atoms as if they were a gas the fraction of atoms with a velocity in the range dV about V_T moving in

a solid angle $d\Omega$, yields the velocity distribution

$$P(V_T)dV_T d\Omega = \left[\frac{M}{2\pi kT}\right]^{3/2} \exp(-\frac{MV_T^2}{2kT})V^2_T dV_T d\Omega. \qquad (II.66)$$

Assuming a monoenergetic beam of neutrons along the target z axis, V_z is the projection of the velocity on the z axis,

$$V_z = V\cos\theta = V\mu \qquad (II.67)$$

and the distribution V_z is,

$$Q(V_z)dV_z = \int_0^1 P(V_z/\mu)d\frac{V_z}{\mu}2\pi d\mu \qquad (II.68)$$

Integrating over μ yields,

$$Q(V_z)dV_z = \left[\frac{M}{2\pi kT}\right]^{1/2} \exp(-MV^2_z/2kT)dV_z. \qquad (II.69)$$

The Breit-Wigner formula is averaged over this distribution to calculate the effective cross section. The z velocity is expressed in terms of the neutron energy and the relative energy of the system to simplify the evaluation of the integral.

$$E = \frac{1}{2}m_R|v_n - V_T|^2 = \frac{1}{2}m_R(v_n^2 + V_T^2 + v_n V_z) \qquad (II.70)$$

Note that V_T is a vector quantity and that v_n is the neutron velocity in the z direction. The V^2_T term can be neglected

for heavy nuclei, because the average target velocity is much smaller than the neutron velocity. Thus,

$$E = E_n - \sqrt{m_v E_n V_z} \tag{II.71}$$

The distribution function can now be rewritten in terms of the relative energy and the neutron energy

$$Q(V_z)dV_z = \left[\frac{M}{2\pi kT}\right]^{1/2} \exp\left[\frac{-M(E - E_n)^2}{(2mE_n)(2kT)}\right]\frac{dE}{2mE_n} \tag{II.72}$$

The single level Breit-Wigner formula for an s-wave neutron is,

$$\sigma(E) = \frac{\sigma_o}{1 + \left[\frac{E - E_o}{\Gamma/2}\right]} \tag{II.73}$$

Defining the Doppler width, Δ,

$$\Delta = \sqrt{\frac{4mE_n kT}{M}} \tag{II.74}$$

and substituting in eq. II.64 the effective cross section becomes

$$\sigma(E_n) = \frac{1}{\Delta\sqrt{\pi}}\int \frac{\sigma_o}{1 + \left[\frac{E - E_n}{\Gamma/2}\right]^2}\exp[-(E - E_n)/\Delta]^2\, dE \tag{II.75}$$

By assuming the 1/v cross section to be nearly constant over

the width of a resonance, the 1/v term σ_o can be taken outside the above integral, and making the following substitutions

$$x = \frac{E_n - E_o}{\Gamma/2} \tag{II.76}$$

and

$$y = \frac{E - E_o}{\Gamma/2} \tag{II.77}$$

$$= \frac{\Gamma}{\Delta} \tag{II.78}$$

Then

$$\sigma(E) = \sigma_o \psi(\xi, x) \tag{II.79}$$

where

$$\psi(\xi, x) = \frac{\xi}{2\sqrt{\pi}} \int \exp\left(\frac{-1/4\,\xi^2 (x-y)^2}{1 + y^2}\right) dy \tag{II.80}$$

This formula (ref. 18) is often called the Voight profile in honor of the man who first studied it (ref. 19). Values of ψ have been tabulated and a file is maintained on line at the City University Computer Facility to calculate effective thermal neutron cross sections.

Bibliography

1. Bethe, Phys. Rev. 47,747(1935)

2.a L. Szilard, Nature,136, 950(1935)

2.b E. Fermi and F. Rasetti, Nuovo Cimento, 12, 201(1935)

3. N. Bohr, Nature, 137,344(1936)

4. P. Marmier and E. Sheldon, "Physics of Nuclei and Particles", Academic Press(1970), vol. II, p.1087

5. G. Friedlander, J.W. Kennedy and J.M. Miller, "Nuclear and Radiochemistry"

6. R.D. Evans, "The Atomic Nucleus", McGraw-Hill(1955)

7. G. Breit and E.P. Wigner, Phys. Rev., 49, 519, 642(1936)

8. P. Marmier and E. Sheldon

9. E. Almaldi, O. D'Agostino, E. Fermi, B. Pontecorvo, F. Rosetti, and E Sigri, Proc. Roy. Soc. (London), A149, 522(1935)

10. A.M. Weinberg and E.P. Wigner

11. C.H. Westcott, "Effective Cross section Values for Well-Moderated Thermal Reactor Spectra", 3rd ed., corrected, AECL-1101, Chalk River Nuclear Laboratories, Atomic Energy of Canada Limited(1970)

12. C.H. Westcott, W.H. Walker, and T.K. Alexander, "Effective Cross Sections and Cadmium Ratios for the Neutron Spectra of Thermal Reactors", Proc. 2nd. Intern. Conf. Peaceful Uses of At. Energy, Geneva, 1958, 16, 70(1959), United Nations, New York.

13. C.H. Westcott, "Effective Cross Section Values for Well-Moderated Thermal Reactor Spectra", AECL-407, Chalk River Nuclear Laboratories, Atomic Energy of Canada Limited(1957).

14. M.J. Poole, J. Nuclear Energy, 5, 325(1957)

15.a T.A. Eastwood, Intern. J. Appl. Radiat. Iso., 17, 17(1966)

15.b T.A. Eastwood and R.D. Werner, Can. J. Phys., 41, 1263(1963)

16. M.F. Elgart, H.L. Finston, R. Rundberg, E.T. Williams, A.H. Bond, E. Yellin, Nucl. Sci. Eng., 58, 291-297(1975)

17. A. Foderaro, "The Elements of Neutron Interaction

Theory", MIT Press,(1971),p. 507

18. T.D. Beynon and T.S. Grant, Nucl. Sci., 17,545(1963)

19. W. Voight, S.B. bayer Akad. Wiss., p.603(1912)

III. Experimental procedures.

Gamma spectra were determined by single parameter pulse height analysis with a 40 cc coaxial Ge(Li) detector. The resolution measured in the system was 1.85 keV fwhm on the ^{60}Co 1332.2 keV gamma which is in excellent agreement with the factory specifications for the detector.

Figure I is a diagram of the counting system consisting of :

1. Ge(Li) detector: The detector is a Princeton Gamma Tech Inc. coaxial Ge(Li) serial number 1024 with a 1.85 keV full width at half height resolution for the 1.332 MeV ^{60}Co gamma ray. The diameter of the crystal is 40 mm, the volume is 50 cc, with a 40 cc active volume and an efficiency of 7.3 percent relative to the efficiency for the 1.33 MeV gamma ray of ^{60}Co at a distance of 25 cm from a 3 inch x 3 inch sodium iodide at 25 cm.

2. Preamplifier: The Princeton Gamma Tech model RG-11 FET input preamplifier is mounted directly onto the cryostat of the detector. The preamplifier integrates the output pulses of the Ge(Li) for presentation to the pulse shaping main amplifier.

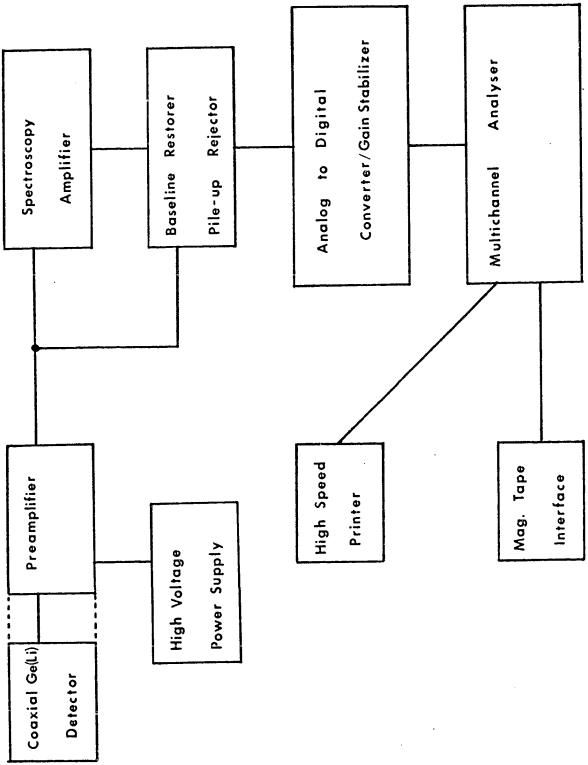

Figure 1. The Counting System

3. Amplifier: The amplifier was a Canberra model 1417 spectroscopy amplifier, which is highly stable (better than $\pm$ 0.075% linearity), has low noise contribution and near optimum Gaussian pulse shaping is achieved with pole zeroed unipolar pulses.

4. Baseline restorer/ Pileup rejector: This unit, a Canberra model 1464, was used for high activity samples to alleviate the problems associated with a high count rate, namely, loss of resolution due to pileup, baseline fluctuation and low frequency noise enhancement (due to pole zero compensation).

5. Pulse height analyser: A 4096 channel Northern Scientific NS-630 multi-channel analyser with a 8192 channel NS-627 ADC was used. The multi-channel analyser had a memory containing 4096 channels each having a capacity of 6 BCD words (a maximum of 999999 counts per channel). The analyser was interfaced for output to a high speed paper tape printer (1200 characters a second), a Wang MOD 7 tape drive, and an analog output to a X-Y recorder. The ADC is a 50 Mhz 13 bit ADC with digital zero level and gain stabilization.

6. Data storage: The analyser is interfaced to a Wang MOD 7 tape drive through a NS-406 readout unit and a NS-406m tape controller. The recorded data has a 9 track IBM

compatible format. The spectra are stored with a predata word identifying the spectrum in BCD; each spectrum is recorded as one record, with a maximum length of 6x4096 bytes plus the six byte predata word. The recording density is 800 bits per inch which makes these tapes incompatible with the City University Computer facility, since the lowest density drives available there are 1600 bpi. The tapes were, therefore, first decoded at the Brooklyn College School of Science Data Acquisition Facility. The operating system of the Data Acquisition Facility, "UNIX", was obtained from Bell Laboratories. A program (see appendix A) to decode the tapes was written in C (a compiler similar to PL1). This special program enabled much more rapid retrieval of data by a factor >100 over existing systems programs.

The gamma spectra were analysed by a computer program "Brutal" written by Gunnik at Livermore Labs. The version used was obtained from Harbottle and Sayres of Brookhaven National Laboratories. "Brutal" analyzes spectra for overlapping peaks and separates them by fitting them to a gaussian distribution and it also determines the energy of the center of the fitted peak. The program finds legitimate peaks in the spectrum by comparing the difference between channels with the minimum error; if the difference is less than $1.5\sqrt{N}$ no peak is found. The shape of each peak is also

checked for the presence of multiple peaks and is rejected if too broad, thus eliminating Compton peaks. Suspect peaks in the final output were starred. Comparison of the computer interpreted spectrum with hand calculation using human judgment as to the significance of peaks (e.g. twice background) gave remarkable agreement. The program made the identification of the peaks and the integration more reliable and faster.

A standard counting geometry was obtained with a two foot lucite tower mounted over the detector. The tower had a rectangular upper portion which was slotted to hold 3 1/8" square aluminum plates. The lower portion was a lucite cylinder milled to fit snuggly over the cryostat of the Ge(Li). The slots were placed at several positions so that the desired counting rate could be achieved with a well defined position (see fig. II). The aluminum mounting plates have 1 1/2 inch diameter holes in the center so that wire sources such as Co-Al flux monitors can be supported by adhesive tape in the center of the plate. Ampoules were supported on a special mounting plate which has a 2 inch diameter solid lucite cylinder attached to the aluminum plate. In the center of the cylinder is a 4 millimeter diameter hole drilled to within 1 mm above the aluminum plate. Sample volumes were taken as nearly identical as possible because the ampoules are mounted vertically.

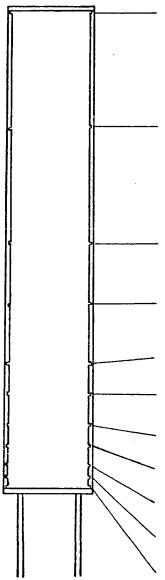

Counting Geometry

Figure II.

Neutron irradiations

Neutron irradiations were performed in both the High Flux Beam Reactor (HFBR) and the Brookhaven Medical Research Reactor (BMRR) at Brookhaven National Laboratories. The Medical Reactor was used because it has a different neutron temperature from the HFBR due to the different reflectors in the two reactors. When it was necessary to obtain a cadmium ratio, a specially designed capsule was required in the in-core and near-core positions of the HFBR due to the extremely high gamma intensity in these positions.

1. The High Flux Beam Reactor (ref. 1,2): This reactor was designed principally for use in neutron diffraction and other experiments requiring intense neutron beams. The reactor has a heavy water reflector to maximize the neutron flux, and this choice of moderator provides a variety of neutron spectra in different irradiation facilities. The HFBR is a tank type, fully enriched (93%) uranium, heavy water moderated, cooled and reflected. Maximum thermal neutron flux is 7.0×10^{14} n/cm^2 sec and 1.6×10^{15} n/cm^{2}sec maximum fast flux. The average moderator temperature is 55 degrees centigrade and the maximum temperature is 182 degrees. The reflector contains 1200 gallons of heavy water and has an average temperature of 57 degrees. The facilities used in this work are V-11, V-14, and V-15, three of the vertical

High Flux Beam Reactor

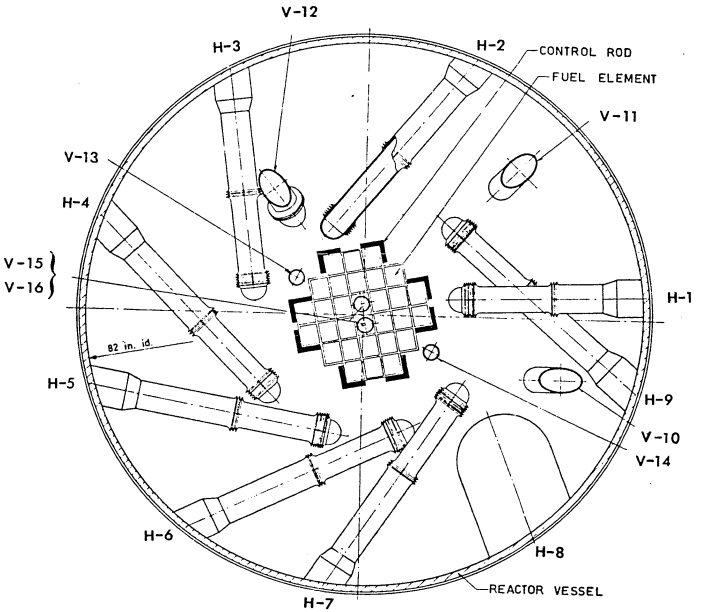

HORIZONTAL SECTION REACTOR HFBR

Figure III

facilities used for the neutron irradiations and are distinguished from the beam tubes labelled H in figure III.

V-11 is a reflector position located about 80 cm from the core edge which is a sufficient distance to render all epithermal flux insignificant with respect to the thermal. This facility is provided with a pneumatic tube so that samples may be introduced in a rabbit. The gamma heating in this position is low and requires no special design for the irradiation container.

V-14 is a core edge facility located about 5 cm from the core with a total neutron flux near maximum at this position. The gamma heating rate is high and the special irradiation capsule described later must be used for irradiations requiring a cadmium shield (ref. 3).

V-15 is an in-core facility located in an empty fuel position. The neutron spectrum calculated for this position is essentially a fission spectrum (ref. 1). There is little moderator in the core due to the compact design so that the thermal component is low for this position. The gamma heating rate in this position is maximal and the capsule described later is required.

The Brookhaven Medical Research Reactor: The medical reactor (ref. 2) designed principally for medical experiments was used in these experiments to provide a radically different

Brookhaven Medical Research Reactor (BMRR)

Figure IV.

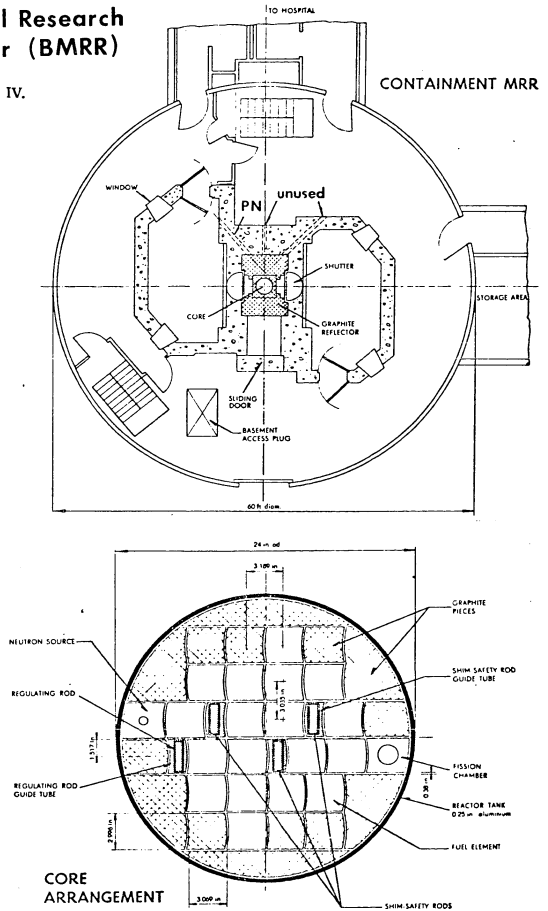

thermal spectrum from the HFBR. The BMRR is a tank type reactor, using fully enriched fuel (>90%) uranium. The core is moderated and cooled with light water, but the reflector is graphite. The average thermal neutron flux is 0.96×10^{13} n/cm^2sec with a maximum of 1.67×10^{13} n/cm^2sec and the average fast flux is 1.5×10^{13} n/cm^2sec. The average temperature of the graphite reflector is 54.5 degrees and the maximum is 77 degrees centigrade. The irradiation facilities available are an in-core position (not shown in fig. IV) and a reflector position called the PN facility. This facility shown in fig. IV is located in the reflector and has a pneumatic tube sample changer. The spectrum in this position is highly moderated so that the epithermal component is small. The neutron temperature in this facility is higher than in the reflector of the HFBR because graphite has a higher absorption cross section than D_2O and therefore hardens the thermal spectrum.

The irradiation capsule

The irradiation capsule shown in fig. V was designed for use in the in-core and near-core positions of the HFBR. The cadmium shield was limited to a length of 2 inches since a larger surface area of cadmium would seriously reduce the operating level of the reactor. The end of the aluminum capsule is welded to an aluminum tube to remove any gas pressure which may build up during the irradiation. The

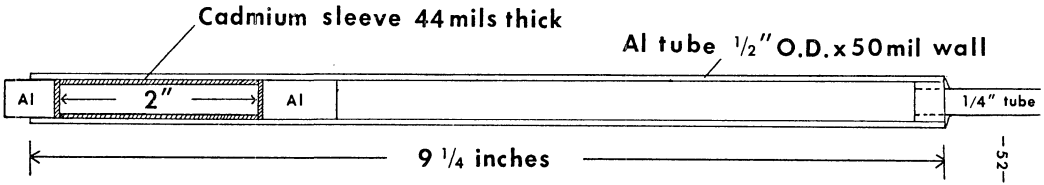

Figure V. The irradiation capsule.

aluminum spacer shown in the center of the capsule separated the bare sample from the cadmium shield and reduced the solid angle exposed to the cadmium hardened spectrum.

Ge(Li) efficiency calibration

An absolute efficiency curve (figure VI) for the Ge(Li) was determined using an N.B.S calibrated ^{60}Co source and a N.B.S. calibrated ^{94}Nb source. Both sources are point sources and were mounted 12.6 cm from the detector on the axis (slot 6 on the standard geometry figure II), the lower energy region of the efficiency curve was obtained by calibration with a ^{116m}In source produced in a 1 cm diameter indium foil irradiated in a neutron howitzer for 4 hours. The intensity of the 137, 417, 818, 1097, and 1293 keV gamma rays of ^{116m}In were calculated from the relative intensities by calibration of the 1293.5 keV gamma ray which is in the region of ^{60}Co gamma rays. The gamma ray intensities and the calculated activities are listed in Table I. An additional calibration point was afforded by using the gamma ray of ^{95m}Nb in a ^{95}Zr source. The determination was made several months after the production of the activity in a neutron irradiation in the Brookhaven H.F.B.R. so that the ^{95m}Nb was in equilibrium.

^{95}Zr beta decays to 3 levels in ^{95}Nb; the subsequent gamma rays emitted in the decay of these levels have ener-

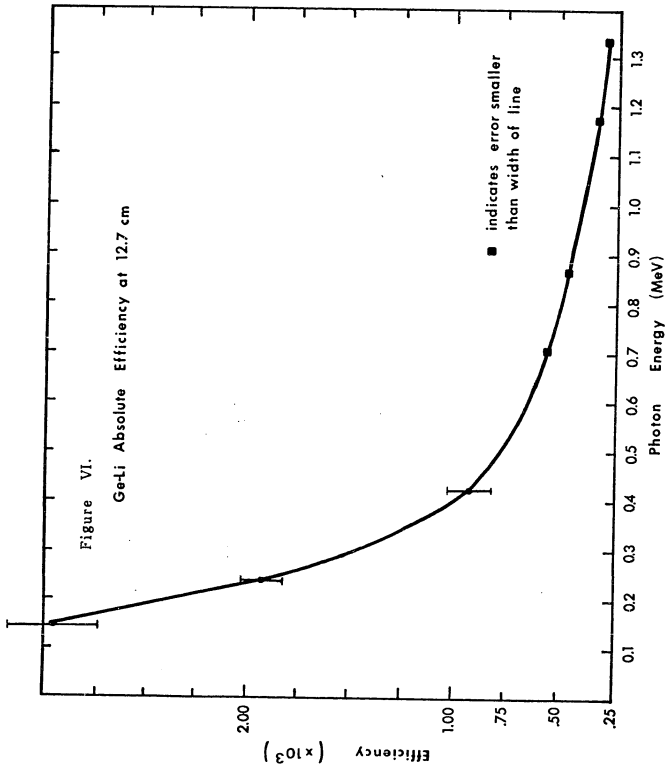

Table I Ge(Li) Efficiency Calibration

nuclide	γ energy	relative intensity	activity cps	absolute dis. rate	efficiency
^{60}Co	1332.5keV	100	18.34	$6.36\ 10^{4}$	$2.88\ 10^{-4}$
	1173.2	100	21.04	"	$3.31\ 10^{-4}$
^{94}Nb	871.1	100	3.41	$7.40\ 10^{3}$	$4.61\ 10^{-4}$
	702.6	100	4.18	"	$5.65\ 10^{-4}$
^{116m}In	1293.5	100	0.60	$^{1}2.01\ 10^{3}$	$2.98\ 10^{-4}$
	1097.5	59.8	0.49	$1.2\ 10^{3}$	$2.98\ 10^{-4}$
	818.7	17.1	0.16	344.	$4.65\ 10^{-4}$
	416.8	40.2	0.73	809.	$9.04\ 10^{-4}$
	137.5	4.9	0.29	98.	$2.95\ 10^{-3}$
^{95}Zr	724.2	100	13.80	$^{2}2.50\ 10^{4}$	$5.52\ 10^{-4}$
^{95m}Nb	235.6	$^{3}.0069$	2.60	$1.95\ 10^{5}$	$1.93\ 10^{-3}$

note 1. Interpolated from ^{60}Co data.
2. Interpolated from ^{94}Nb data.
3. Relative to ^{95}Zr.

gies of 756, 724 and 235 keV respectively (ref. 4). The 235 keV gamma is emitted from the internal transition of a 90 hour isomer of ^{95}Nb. The ratio of 235 keV intensity to 724 keV intensity was calculated by assuming a steady state equilibrium so that the relative activity of ^{95m}Nb is equal to the branching ratio for the beta decay of ^{95}Zr. The branching ratios to the 756, 724 and 235 keV levels are 54.1, 44.7, and 1.2 percent respectively (ref. 5). The 724 keV transition is M1 and E2 and has a conversion ratio of $e_K/\gamma = .0011$. The 235 keV transition has been assigned to an M4 transition and is highly converted, $\frac{\gamma}{e + \gamma} = .259$, thus the ratio of relative intensities is 6.9×10^{-3} .

Bibliography

1. H.J.C. Kouts, "Neutron Physics of and with the High-Flux Beam Reactor", BNL-664, Brookhaven National Laboratory (1961).

2. " Directory of Nuclear Reactors ",International Atomic Energy Agency, Vienna(1959).

3. J.J. Floyd, Private communication.

4. Lederer, Hollander, and Perlman, "Table of Isotopes", 6th Ed.

5. R.H. Filby, A.I. Davis, K.R. Shah, G.G. Wainscott, W.A. Haller, W.A. Cassatt, "Gamma Ray Energy Tables for Neutron Activation Analysis", WSUNRC-97(2), Washington State University (1970).

IV. Applications

Reactor spectra -experimental

The neutron energy distribution

Although only two components of the neutron spectrum were heretofore considered, the neutron energy distribution is divided into three parts (ref 1.); (1) the fission spectrum; (2) slowing down distribution; (3) thermal neutrons. The fast neutrons (several MeV) emitted in the fission of uranium are slowed in reactors by a moderator until they reach thermal equilibirium. The fast neutrons (energy > 1 MeV)present in a reactor spectrum are largely fission neutrons which have escaped slowing down; the contribution to the fast neutrons from reactions other than the primary fission is small. The shape of the fission spectrum of ^{235}U has been measured by (n,p) scattering (ref. 2,3) and time of flight techniques (ref. 4). The flux density per unit density is represented by the following functions:

$$N(E) = 0.484\exp(-E)\sinh\sqrt{2E} \quad \text{(ref.2)}, \tag{IV.1}$$

$$N(E) = 0.4527\exp\left(\frac{-E}{0.965}\right)\sinh\sqrt{2.29E} \quad \text{(ref.3)}, \tag{IV.2}$$

$$N(E) = 0.77E^{1/2}\exp(-0.776E) \quad \text{(ref.4)}. \tag{IV.3}$$

However, fission spectra determined from threshold detectors (nuclides having zero cross section below a certain energy or threshold) disagree with these functions casting some doubt as to the validity of the form of the spectrum or the threshold method.

The slowing-down spectrum covers the energy range of ~.1 eV to 1MeV and is characteristically $\phi(E) = k/E$ where k is a constant. The validity of the 1/E function has been tested using cadmium ratios of neutron absorber with epithermal resonances.

The thermal distribution is generally approximated by a Maxwell-Boltzman distribution which has been shown to be valid for nuclides with a thermal resonance above .0253 eV (Ref. 5.). The effective neutron temperature can be measured using an absorber having a resonance in the thermal region such as ^{176}Lu for which the variation of the effective cross section with temperature has been calculated.

The neutron spectrum in various positions of the High Flux Beam Reactor at Brookhaven National labs has been measured using the above approximations so that the effective cross sections subsequently measured can be interpreted correctly to yield as much information as possible, e.g. thermal cross section, resonance integral, etc.

The applicability of the Westcott convention for measuring the thermal neutron flux in various irradiation positions in the high-flux beam reactor (HFBR) at Brookhaven National Laboratory was investigated first. This reactor provides a high flux of both energetic neutrons [capable of producing (n,2n), (n,p), etc. reactions] and thermal neutrons. It was necessary to test the applicability of the Westcott convention and to determine the intensity of the fast flux in order to find reactor positions suitable to the method described earlier in section II.

A preliminary experiment was performed to determine the Westcott parameters for three irradiation positions in the HFBR: at the center of the core (V-15); at a horizontal distance of 5 cm from the perimeter of the core (V-14); and in the reflector region, 50 cm from the core perimeter (V-11).

The target materials were ^{59}Co and ^{198}Au for which the values of σ_o, I', and s_o are known (refs. 6,7). They were irradiated in the form of 0.53% cobalt in aluminum wire (0.015-in. diam), provided by B.N.L. , and 0.093% gold in aluminum wire (0.020-in. diam.) purchased from Reactor Experiments Inc. Pure nickel wire, also provided by B.N.L., was also irradiated to enable an approximate determination of the fast flux (>1 Mev) via the $^{58}Ni(n,p)^{58}Co$ reaction. A sample consisted of one segment each of cobalt-aluminum,

gold-aluminum (sealed in quartz), and nickel wires wrapped together in aluminum foil. The self-shielding of these samples was negligible (Ref. 8,9); for example the self-attenuation in the gold-aluminum wire was <0.1%. The weights of samples (i.e. flux monitors), the irradiation positions, etc. are summarized in Table II.

Table II. Flux monitor weights

facility		Au-Al(mg.)	Co-Al(mg)	Ni(mg.)
V-15	bare	4.42	7.63	24.23
	shielded	4.50	7.64	24.40
V-14	bare	2.34	7.69	25.02
	shielded	2.40	7.70	25.73
V-11	bare	2.30	7.65	25.27
	shielded	2.47	7.62	25.30

The irradiation container was an aluminum tube 1/2 in. o.d.x 9 1/2 in. long in which the samples were placed end to end. Two samples were placed directly in the tube. The remaining samples were first placed in a cadmium sleeve with walls 0.045 in. thick that was capped with cadmium at both ends and then force-fitted into the aluminum tube to ensure good thermal contact. The overall length spanned by all the sample tubes was only 4 in; thus there was no significant variation in the flux (Ref. 10) over the length of the sample.

It was not possible to irradiate all three containers simultaneously since the reactor could not tolerate so much extra cadmium in and near the core. The first two containers were irradiated simultaneously in the V-14 and V-11 positions and the third was loaded into the core position immediately after the removal of the first two to minimize the effect of any changes in the reactor spectrum during the 21-day operating cycle.

The samples were irradiated for 8 h. to provide a relatively short irradiation necessary to prevent burnup of ^{58}Co (half life = 71.3 d) activity and to limit production of ^{198}Au (half life = 2.698 d) . On the other hand, the irradiation time had to be long enough so that the loading procedure (15 min minimum necessitated by the appreciable adjustment of the control rods as the sample is inserted or withdrawn) did not significantly effect the total flux experienced by the sample.

Experience has shown that the flux at a given position tends to vary over the course of an operating cycle, and in a Brookhaven memo (Ref. 11) it was reported that the flux varies approximately 10% and is an unpredictable function with respect to time. Furthermore, in two separate trials in V-14, we obtained a value of R_{Cd} for ^{60}Co equal to 7.7 in March 1973 and a value of 15 for the same ratio in August of that same year. The difference was attributed to

changes in fuel enrichment and the age of the fuel elements. Thus it is imperative that the pertinent Westcott parameters be measured for each and every irradiation.

The activities of ^{60}Co, ^{199}Au, and ^{58}Co in the sample were determined by means of gamma-ray spectroscopy using a Ge(Li) detector. Absolute activities were obtained for ^{60}Co by calibrating the system with a ^{60}Co standard source obtained from the National Bureau of Standards (NBS). The results are shown in Table I.

Neutron temperature measurements

The neutron temperatures were determined in the Brookhaven Medical Research Reactor and the V-11 facility of the H.F.B.R. using lutetium as temperature monitor. ^{176}Lu has a strong resonance, σ_o = 1920 barns at an energy of 0.142 ev with a width of .060 eV. The effective thermal cross section varies markedly with neutron temperature in the range of temperatures normally found in most reactors.

The lutetium targets were prepared from 99.995% Lu_2O_3. Although lutetium oxide when freshly prepared has been reported as soluble in most mineral acids, the Lu_2O_3 would not dissolve in any strong mineral acids and required treatment by potassium acid sulfate fusion. A sample consisting of 90.65 mg of Lu_2O_3 was covered by 3 grams of potassium pyrosulfate and heated until all visible traces of

Table III

Westcott parameters in HFBR irradiation facilities

Position	Au		Co		nv_o	Relative
	R_{Cd}	r'	R_{Cd}	r'	(n/cm^2-sec)	fast flux
In core (V-15)	1.03	1.1 $\pm$0.3	1.60	0.60 $\pm$0.01	-	1.00
Near core (V-14)	1.77	0.069 $\pm$.001	7.79	0.068 $\pm$.001	4.1×10^{14}	0.28
Reflector (V-11)	112	4.9×10^{-4} $\pm 0.5 \times 10^{-4}$	1240	4.0×10^{-4} $\pm 0.5 \times 10^{-4}$	2.0×10^{14}	$<10^{-4}$

the lutetium oxide had dissolved and then heated an additional 15 minutes. The soluble lutetium sulfate was then dissolved in dilute sulfuric acid and diluted to 1 liter.

A 50 microliter aliquot of the stock solution was deposited on a high purity aluminum foil, dried in a vacuum desiccator, folded to fit in a quartz ampoule, and sealed. The area of the folded foil is approximately .01 cm^2 so that the thickness of the lutetium target was 4.53×10^{-4} grams per cm^2 ^{176}Lu, and the mass attenuation coefficient at the resonance maximum is μ=6.57 cm^2 per gram so self shielding effects could be neglected.

A pair of samples one in a cadmium shield and one bare were irradiated simultaneously in the PN tube (the pneumatic tube facility see fig IV) of the Brookhaven Medical Research Reactor (BMRR) for 1 hour. The activity of ^{177}Lu was measured by counting the 208 keV gamma, which showed a half life of 6.76 days in close agreement with the accepted value 6.74 days. The activity extrapolated back to the end of irradiation was 15.3 cps, yielding an absolute disintegration rate of 6.47×10^4 dps after applying appropriate correction factors. The neutron fluence was determined from the measured activity in Co-Al monitors packed with the lutetium targets in the irradiation capsule.

The neutron temperatures for the HFBR and BMRR are

Table IV

^{176}Lu g-values vs neutron temperature

Temperature (^{o}K)	Westcott g-value									
173.0	1.055	1.059	1.063	1.067	1.071	1.075	1.080	1.084	1.088	1.092
183.0	1.097	1.101	1.105	1.110	1.114	1.118	1.123	1.127	1.132	1.137
193.0	1.141	1.146	1.150	1.155	1.160	1.165	1.170	1.174	1.179	1.184
203.0	1.189	1.194	1.199	1.204	1.209	1.214	1.220	1.225	1.230	1.235
213.0	1.241	1.246	1.251	1.257	1.262	1.268	1.273	1.279	1.284	1.290
223.0	1.295	1.301	1.307	1.312	1.318	1.324	1.330	1.335	1.341	1.347
233.0	1.353	1.359	1.365	1.371	1.377	1.383	1.389	1.395	1.402	1.408
243.0	1.414	1.420	1.426	1.433	1.439	1.445	1.452	1.458	1.465	1.471
253.0	1.478	1.484	1.491	1.497	1.504	1.510	1.517	1.524	1.530	1.537
263.0	1.544	1.550	1.557	1.564	1.571	1.577	1.584	1.591	1.598	1.605
273.0	1.612	1.619	1.626	1.633	1.640	1.647	1.654	1.661	1.668	1.675
283.0	1.682	1.689	1.696	1.703	1.711	1.718	1.725	1.732	1.739	1.747
293.0	1.754	1.761	1.768	1.776	1.783	1.790	1.798	1.805	1.812	1.820
303.0	1.827	1.834	1.842	1.849	1.857	1.864	1.871	1.879	1.886	1.894
313.0	1.901	1.909	1.916	1.924	1.931	1.939	1.946	1.954	1.961	1.969
323.0	1.976	1.984	1.991	1.999	2.006	2.014	2.022	2.029	2.037	2.044
333.0	2.052	2.059	2.067	2.075	2.082	2.090	2.097	2.105	2.112	2.120
343.0	2.128	2.135	2.143	2.150	2.158	2.166	2.173	2.181	2.188	2.196
353.0	2.203	2.211	2.219	2.226	2.234	2.241	2.249	2.257	2.264	2.272
363.0	2.279	2.287	2.294	2.302	2.309	2.317	2.324	2.332	2.339	2.347

reported in Table IV . The facilities labeled H-1, H-2, and H-4 (see fig. IV) are horizontal beam ports in which the temperatures were also measured with Lu monitors by the BNL staff (Ref. 12). The beam port H-4 extends into the reflector approximately 20 cm. from the core edge. H-1 is directed toward the core and is approximately 10 cm. from the core edge. The higher temperature for H-1 over H-4 and H-2 is due to the closer proximity to the core (less moderation) and also a probable larger anisotropic contribution of harder neutrons. The temperature for V-11 is in good agreement with the Brookhaven data. There is no data for comparison in the Brookhaven Medical Research Reactor, but the value 55 ^{o}C is only slightly higher than the ambient temperature and is in agreement with temperature measurements in other graphite reflector reactors.

The cold neutron temperatures measured in the HFBR are characteristic of heavy water moderated reactors and are due to an effect called "diffusion cooling". This effect first proposed by Von Dardel (Ref. 13) is due to the preferential leakage of high energy neutrons from regions where the spatial variation of the flux has a positive curvature. The higher temperatures observed in graphite moderated reactors are due to spectrum hardening by graphite.

Table IV. Neutron Temperature Measurements

Reactor	facility	T(^{o}K)	T(^{o}C)
HFBR	H-1	247	-26
"	H-2	237	-36
"	H-4	236	-37
"	V-11	243	-30
BMRR	Reflector	328	55

Sodium-22 and iodine-126

Following the completion of the experiment described in section IIIA.2, irradiations were made to determine the cross sections of ^{22}Na and ^{126}I. These nuclides were produced by (n,2n) reactions in samples of high-purity sodium carbonate and lead iodide respectively.

A 0.14686 gram sample of 99.98% purity Na_2CO_3 (Thorn Smith analyzed reagent) was irradiated in the unshielded portion of the capsule and a 0.15647 gram sample in the cadmium shielded portion. A 0.02827 gram sample of 99.9999% pure PbI_2 (Apache Chemical Co.) was irradiated in the unshielded portion of the capsule and 0.02263 grams in the cadmium shielded portion. The samples were placed in tubes of high purity quartz (3mm o.d., 2cm long), dried to constant weight, and sealed. These ampoules, each accompanied by a segment of cobalt-aluminum flux wire, were individually

wrapped in high purity aluminum foil the weights of the flux wires were 15.59 mg and 16.27 mg in the bare and cadmium shielded capsules respectively.

The first irradiation, to obtain R_1 [Eq. II.53], was performed in V-14, which had been shown suitable for production and burnup in the preliminary experiment; the sample was irradiated for 8 days.

The activities in the unopened quartz tubes and the flux wires were measured with the Ge(Li) detector system. The activity of each nuclide was determined by integration of a prominent gamma-ray peak: 0.386 Mev for ^{126}I, 0.511 and 1.25 Mev for ^{22}Na, and 1.33 Mev for ^{60}Co. Since the method depends on a relative measurement, it is not necessary to know either the absolute intensity of the gamma-ray or the fraction of decays giving the gamma ray. The ratios in table II are the averages of a number of individual measurements.

The sodium activity was measured via the 1.275 MeV gamma of ^{22}Na to eliminate ambiguity as to the origin of the gamma ray. The samples were counted over a period of one month and no significant deviation from the accepted half life of ^{22}Na was observed. A total of 421460 counts was accumulated for the bare sample in a time period of 5.7×10^5 seconds live time. The activity of the ^{126}I activity in the unshielded sample corresponds to the accumulation of 270282

counts over $7x10^4$ seconds. The cadmium shielded samples accumulated 317587 counts in $9x10^4$ seconds and 288036 counts in $7x10^4$ seconds for the ^{22}Na and ^{126}I samples respectively.

The respective fluxes were monitored with Co-Al flux wires which weighed 15.59mg for the bare and 16.27 mg for the cadmium wrapped sample. The absolute disintegration rate was determined by comparison with a NBS calibrated ^{60}Co source and the results are reported in table VI.

Following the determination of R_1, the samples, each accompanied by a fresh cobalt monitor, were reirradiated in the same configuration used in the initial irradiation. Due to scheduling difficulties, it was not possible to irradiate in V-11. Therefore the sample was placed in the V-14 thimble and withdrawn to a distance from the core corresponding to that in V-11. This position was shielded somewhat by the upper control rods in the operating position and consequently the thermal flux was lower than that in the V-11 position (compare nv_o in Tables I and III). The samples were irradiated in this position for 10 days, and removed from the reactor, cooled, and the activity ratios (R_2) were determined as described above.

This second irradiation corresponds to a normal burnup experiment in which a cadmium-shielded sample of ^{22}Na is also irradiated. Although the samples were in a well

thermalized irradiation position, we feel that this procedure is an advisable precaution in view of the variability of the flux in research reactors and that the reliability of the result is improved since certain factors cancel in taking the ratio. The first irradiation, of course, is for the purpose of determining the resonance integral.

Results

The first irradiation yielded ratios R_1 of 4.23 and 1.63 for ^{22}Na and ^{126}I respectively. These results plus the measured flux parameters permit solution of equation II.53 . A graph of the solutions to equation II.53 is shown in figure IX, and the minimum cross sections estimated from this plot by assuming zero resonance integrals are 1.6×10^4 and 3.6×10^3 barns for ^{22}Na and ^{126}I respectively.

Table VI Reactor parameters during ^{22}Na experiment

Irradiation	Position	nv_o	r'
1	V-14	5.02×10^{14}	0.0903
		$\pm .05 \times 10^{14}$	$\pm$.0002
2	V-14(raised)	0.945×10^{12}	.0342
		$\pm .009 \times 10^{12}$	$\pm$.0001

The second irradiation in V-14 (raised) position of

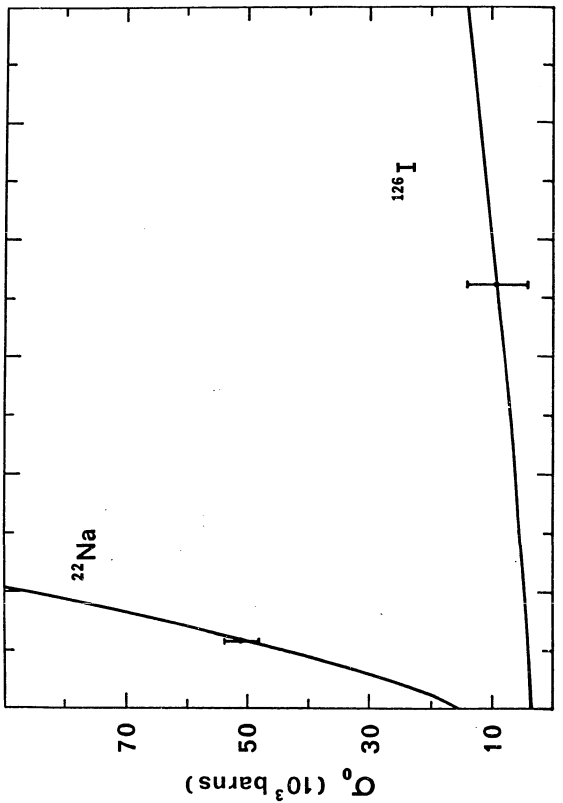

Figure VII. ^{22}Na and ^{126}I σ_o vs s_o

the HFBR yielded a reduced flux for reasons discussed previously, and a reduced epithermal index. Further production of ^{22}Na and ^{126}I can be assumed insignificant in this position since the fast flux drops off more rapidly than the epithermal flux. The second ratio R_2 was 7.52 and 1.76 for ^{22}Na and ^{126}I respectively yielding thermal cross sections from equation II.61 of 5.11×10^4 and 8.9×10^3 barns respectively.

Table VII Results for ^{22} Na and ^{126}I

Nuclide	R_1	R_2	s_o	σ_o(barns)	Σ'
^{22}Na	4.77	7.52	2.3	5.11×10^4	1.0×10^5
	± 0.09	± 0.08	± 0.2	$\pm 0.31 \times 10^4$	$\pm 0.1 \times 10^5$
^{126}I	1.63	1.76	-	9.0×10^3	-
	± 0.01	± 0.09	-	$\pm 5.0 \times 10^3$	-

Cerium-139

Separated isotope ^{142}Nd was irradiated in the near-core facility of the HFBR to produce fast neutron products. It was necessary to use Nd depleted in ^{146}Nd to prevent the production of a large quantity of ^{147}Nd by neutron absorption of ^{146}Nd. The possible fast neutron reactions are $^{142}Nd(n,2n)^{141}Nd$ (half life = 2.46 hr.), $^{142}Nd(n,p)^{142}Pr$

(half life = 19.16 hr) and $^{142}Nd(n,\alpha)^{139}Ce$ (half life = 38 days). Only ^{139}Ce activity was observed because the cool down period required before unloading the irradiation capsule is a minimum of 2 days. Thus the shorter lived isotopes decayed to insignificant levels.

The samples of separated isotope ^{142}Nd consisting of 61.63 mg. and 65.86 mg of Nd_2O_3 were irradiated in cadmium shielded and bare capsules, respectively, in the V-14 facility of the HFBR for 2 days. The gamma ray spectra were surveyed for nuclides produced by fast neutron reactions (n,2n or p or α etc.) and only ^{139}Ce was observed. The Q-value for this reaction is 6.7 MeV so there is no threshold and the barrier for the alpha particle is 15.4 MeV. The effective cross section for production of the cerium activity is therefore expected to be small. The gamma ray spectrum also contained gamma rays identified as ^{141}Ce which could only result from the activation of trace quantities of Ce in the ^{142}Nd sample. It is possible to estimate the effect of trace Ce on the cadmium ratio of ^{139}Ce using the known cross sections for stable Ce. The gamma ray spectrum of ^{139}Ce consists of a single gamma ray with an energy of 166 keV and the spectrum of ^{141}Ce consists of a gamma ray at 145 keV. The ^{139}Ce gamma ray has a conversion ratio e/γ of .24; the ^{141}Ce gamma ray is more highly converted and has a conversion ratio of .44 . The relative detector efficiency at

these energies are 2.83×10^{-3} and 2.67×10^{-3} for the 145 and the 166 keV gamma rays respectively. The observed activities for these nuclides in the bare sample were .172 cps for ^{139}Ce and 2.43 cps for ^{141}Ce. Therefore the ratio of ^{139}Ce to ^{141}Ce activity based on the above data is $5.3 \times 10^{-2} \pm .1 \times 10^{-2}$. The activity ratio calculated from the cross section data of stable Ce is given by the expression:

$$\frac{A_{139}}{A_{141}} = \frac{\sigma_{138} N_{138} \left(1 - \exp(-\lambda_{139} t) \right)}{\sigma_{140} N_{140} \left(1 - \exp(-\lambda_{141} t) \right)}$$

The ratio for a 2 day irradiation is 1.3×10^{-3} as calculated from the natural isotopic abundance of cerium, 88.5 percent ^{140}Ce and 0.26 percent ^{138}Ce, the thermal cross cross sections which are .57 and 1.1 barns respectively and the respective half lives of 32.51 days for ^{141}Ce and 137.5 for ^{139}Ce. Thus the effect of trace concentrations of cerium is estimated to be 2.5 percent. The actual contamination is expected to be less because the sample is separated isotope ^{142}Nd and since the mass of ^{140}Ce is closer to the mass of the neodymium isotope, a less than natural abundance of ^{138}Ce is expected. Therefore the observed cadmium ratio for ^{139}Ce can be used to estimate the thermal cross section.

Results

The cadmium ratio of ^{139}Ce, 0.886 $\pm$.024, is far lower than expected. If the ratio is corrected for the at-

tenuation of fast neutron flux in the cadmium shield assuming 95.8 percent transmission of fast neutrons (based on the ^{54}Mn cadmium ratio) the ratio becomes 0.982 $\pm$.034 which is consistant with a ratio of 1.00. This indicates a smaller cross section than the method can detect. The detectable limit for the cross section is 500 barns assuming a maximum cadmium ratio of 1.02 based on the above uncertainty and the estimate of contamination.

Yttrium-88

Yttriun has only one stable isotope ^{89}Y and the (n,Y) product ^{90}Y (half life = 64 hour) is short lived so the production of ^{88}Y by a (n,2n) reaction should only be observed after a sufficient cool-down period. The Q-value is -11.9 MeV so that the threshold is 12 MeV.

Samples of Y_2O_3 (99.9999 % Apache Chemical) weighing 5935 mg and 64.68 mg were sealed in quartz ampoules and irradiated in cadmium wrapped and bare capsules, respectively, for 2 days in the V-14 facility of the HFBR. After a one month cool down period the sample was counted for two days and no significant ^{88}Y activity was observed. Thus the (n,2n) cross section is too small to produce significant ^{88}Y activity. Since the fast neutron flux was not monitored, no estimate of the (n,2n) effective cross section is available, although the cross section must be less than 1 millibarn.

Rhenium-184

The nuclide ^{184}Re was produced by the following reaction:

$$^{185}Re(n,2n)^{184}Re.$$

by irradiating .24908 grams and .28539 grams of rhenium metal powder (99.95 % Apache Chemical Inc.) sealed in quartz ampoules. These samples, with and without cadmium shields, respectively, were exposed to the reactor flux in the V-14 facility of the HFBR. The cadmium ratio for ^{184}Re determined by comparing the intensities of the .792 and .903 MeV gamma rays in the respective samples was 1.21. The graph in figure X is a plot of the roots of equation II.53 for the above cadmium ratio. The slope is small so that the estimated cross section should be should be close to the actual thermal cross section since the s_c is rarely large (for s_o to be large there must be many resonances at low energy). The thermal cross section estimated from this data assuming no epithermal resonances was 7×10^3 barns.

A second irradiation was made to determine the a unique solution for the thermal cross section. The samples were irradiated for 2 days in the V-12 facility of the HFBR. The samples were then counted over a period of 4 weeks and the new ratio was 1.77. The half lives were also monitored (the data is shown in figure XI) and the results are 37.

Figure VIII. ^{184}Re decay curve irradiation 1.

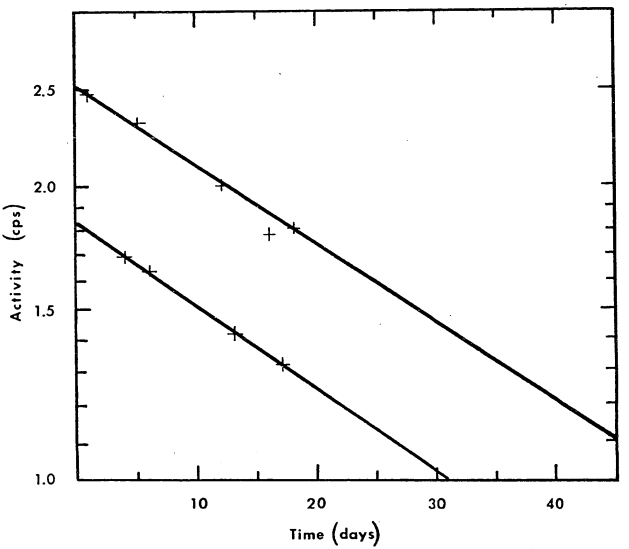

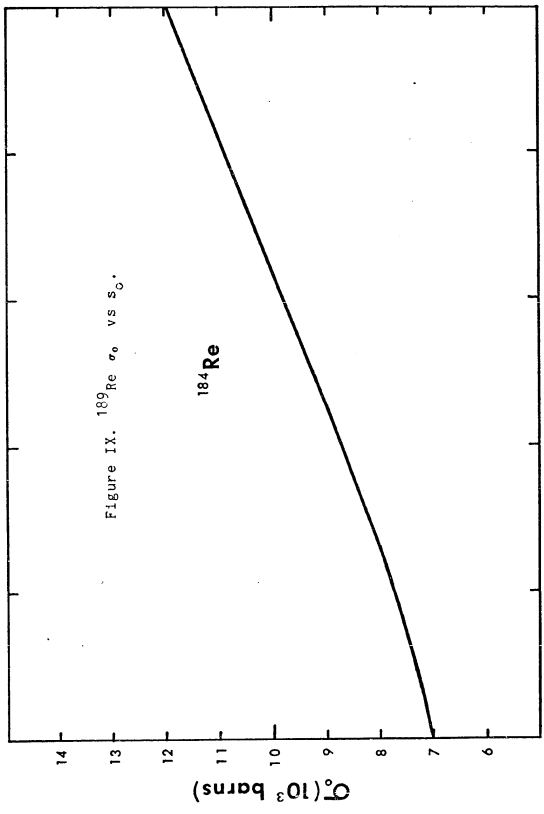

Figure IX. ^{189}Re σ_o vs s_o.

Figure X. ^{184}Re decay curve irradiation 2.

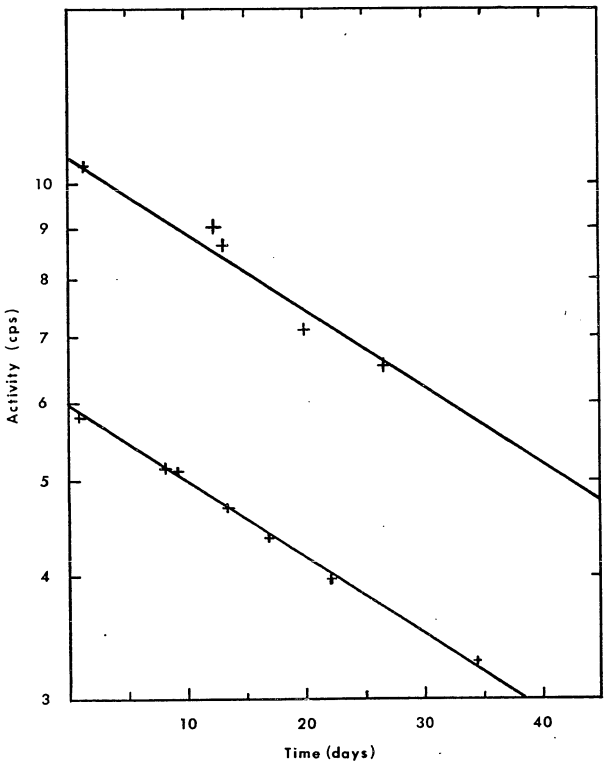

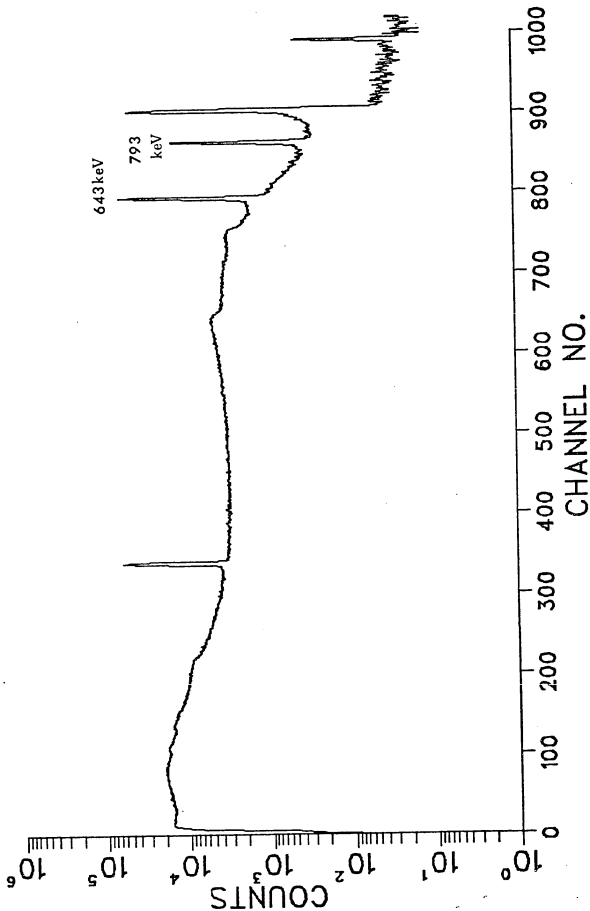

Figure XI. ^{184}Re Gamma Ray Spectrum.

and 38. days respectively. The large error is due to an increase in background activity in the samples.

Results

The ratio of ratios for ^{184}Re is 1.46 and the neutron fluence for the second irradiation is $2.07 \times 10^{19} n/cm^2$. The thermal cross section calculated from equation II.61 is 8.94×10^3 barns. The Westcott s_o is therefore 12.4 as determined graphically from the plot in figure IX. These results are not corrected for neutron spectrum hardening since by assuming g=1 it is also assumed that there is no variation in the cross section with hardening, for ^{185}Re, i.e. the variation parallels that of the ^{59}Co flux monitor.

Tantalum- 182

The nuclide ^{182}Ta was produced in rhenium targets by the reaction:

$$^{185}Re(n,\alpha)^{182}Ta$$

There is no direct way of assuring no contribution from tantalum impurity in the rhenium target. However, the large cadmium ratio indicates that any such contribution is not significant. The calculated cadmium ratio for ^{182}Ta produced by (n,Y) on ^{181}Ta based on literature values for the cross section of ^{181}Ta is 1.12. The ratio is greater than

one because the ^{181}Ta has a much larger resonance integral than thermal cross section and also ^{182}Ta has very large thermal cross secton so that the bare sample will saturate at a lower activity than the cadmium shielded sample. This calculation is only approximate since corrections for shielding by the rhenium were not considered; shielding by the rhenium would tend to lower the burnup in the bare sample. Thus this ratio is maximum.

The cadmium ratio for ^{182}Ta was 1.51 $\pm$.06, the minimum cross section is therefore $1.47 \times 10^3 \pm .14 \times 10^3$, assuming no epithermal resonances, in good agreement with the actual cross section 8.6×10^3 barns. The neutron temperature in the H-1 facility of the HFBR has been determined to be -26 degrees Centigrade and the neutron temperature in the V-14 facility can be assumed close to that in the H-1 beam tube since the distance from the core is nearly equal, thus the g-value at this temperature is approximately 1.5.

The second irradiation yielded no additional information because the background activity in the sample increased so that no significant ^{182}Ta activity could be observed.

The production of ^{182}Ta activity via an (n,α) reaction was interesting because a cheap method of producing carrier free ^{182}Ta would be useful since ^{182}Ta has been pro-

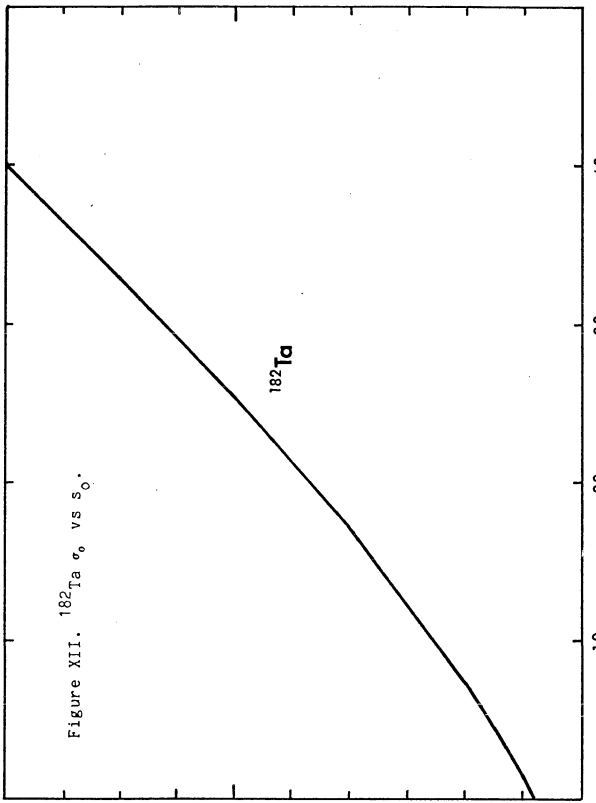

Figure XII. ^{182}Ta σ_o vs s_o.

posed as a neutron temperature monitor. This experiment showed that ^{182}Ta can be produced via this reaction in a reactor flux, but under these far from optimal conditions the production was not significant. However, irradiation in the in-core facility with a cadmium shield to lower the burnup could improve the yield.

Manganese-54

The nuclide ^{54}Mn was produced in MnO_2 targets exposed to a reactor flux in the near core position of the HFBR by an (n,2n) reaction;

$$^{55}Mn(n,2n)^{54}Mn$$

Two samples of MnO_2 (99.999% Apache Chemical Inc.) weighing 50.78 and 24.49 milligrams respectively were sealed in quartz ampoules, were irradiated as a cadmium wrapped and a bare sample in the V-14 position of the HFBR for 2 days.

A cadmium ratio for ^{54}Mn of 0.958 $\pm$0.009 (95% confidence) was determined by counting the 865 keV gamma ray of ^{54}Mn for a total of 641721 and 298111 counts in the cadmium wrapped and bare samples, respectively. The ratio indicates a 4 percent decrease in flux through the cadmium shield due to scattering and absorption, in good agreement with the ratio, 0.977, estimated from the total cross section of cadmium at 5 MeV (4.1 barns) assuming an anisotropic flux on a

45-mil cadmium slab. If the ratio is assumed to be 5% greater than one the minimum the cross section would be about 1000 barns. Thus the low ratio observed shows no unusual deviation from the previous estimate of less than 40 barns for the cross section of ^{54}Mn (Ref. 14).

The thermal flux of 4.06×10^{14} n/cm^2sec and epithermal index of 0.077 in this experiment is the same as reported in the rhenium experiment.

Zirconium-94

A sample of ZrO_2 was irradiated in the V-11 position of the HFBR to measure the thermal cross section of ^{94}Zr. Zirconium is a structural material in planned thermal breeder reactors, thus the cross section of zirconium isotopes are critically important to the design of these reactors.

A sample of ZrO_2 (Specpure United Mineral and Chemical Co.) weighing 82.52 milligrams was sealed in a quartz ampoule and irradiated for one hour in the V-11 facility of the HFBR. The number of ^{94}Zr atoms in the sample was 7.01×10^{19} based on a isotopic abundance of 17.40 percent. The resulting activity showed a gamma peak at 723.9 keV with a half life of 59.5 days in good agreement with the accepted value. The activity for the counting position used was

48.76 cps on 9:34 August 22, 1977. Extrapolating back to the time of irradiation, 3:30, on August 19, 1977, gives an activity of 50.00 cps . Using the efficiency calibration for the Ge(Li) (see fig. VI) the absolute activity is therefore 9.06×10^4 dps. The absolute disintegration rate is 1.85×10^5 since 49 percent of the decays go to the level giving 723.9 keV gamma ray. The neutron fluence was 4.0×10^{17} n/cm^2 based on Co-Al flux measurements. Thus the thermal cross section is 52 millibarns, in good agreement with previous determinations. This value is, however lower than the total cross section at 2200 meters/second and measurment of the thermal cross section of ^{95}Zr using isotope separated ^{96}Zr and producing ^{95}Zr by an (n,2n) reaction in an experiment as in the previous sections would show if there is significant burnup of ^{95}Zr.

^{22}Na - thermal resonance

The result of the ^{22}Na experiment was somewhat high although not out of the range of previously determined values but disagreed with some of the more recent measurements (see Table XI). An experiment identical to that of Sims (Ref. 16) was performed in the HFBR using carrier-free ^{22}Na to determine whether this was due to some unknown experimental error or whether there was a reactor dependence in addition to those treated by the Westcott convention This

experiment is a simple burnup experiment in which the activity of the ^{22}Na is measured before and after irradiation to determine the depletion rate of the radionuclide. The results of this experiment were in good agreement with the previous measurement and thus prompted another experiment of the same type in the Brookhaven Medical Research Reactor to determine if the difference is due to the different reflector in the reactors used by Sims, and by Werner and Santry, which both have graphite reflectors as does the BMRR.

Samples of carrier-free ^{22}Na were prepared by diluting ^{22}Na (carrier-free obtained from ICN) with dilute hydrochloric acid and pipetting about .2 ml into 3mm diameter quartz tubes. These were then evaporated in a vacuum desiccator and the dried samples sealed. The samples were counted in slot #8 of the standard geometry. The ^{22}Na activity in each of the samples was approximately 2 microcuries. Two samples were counted until the accumulated counts in each sample was over 1 million for the 1.275 MeV gamma ray so the statistical error in counting is .3% (95 percent confidence limit). Two samples having activities of 7.38 cps and 9.26 cps were irradiated with and without cadmium shields, respectively , in th V-11 facility of the HFBR for 24 hours; the ratio before irradiation was $1.254 \pm .007$.

After irradiation in the HFBR the samples were again counted until the accumulated counts were over 2.5 million

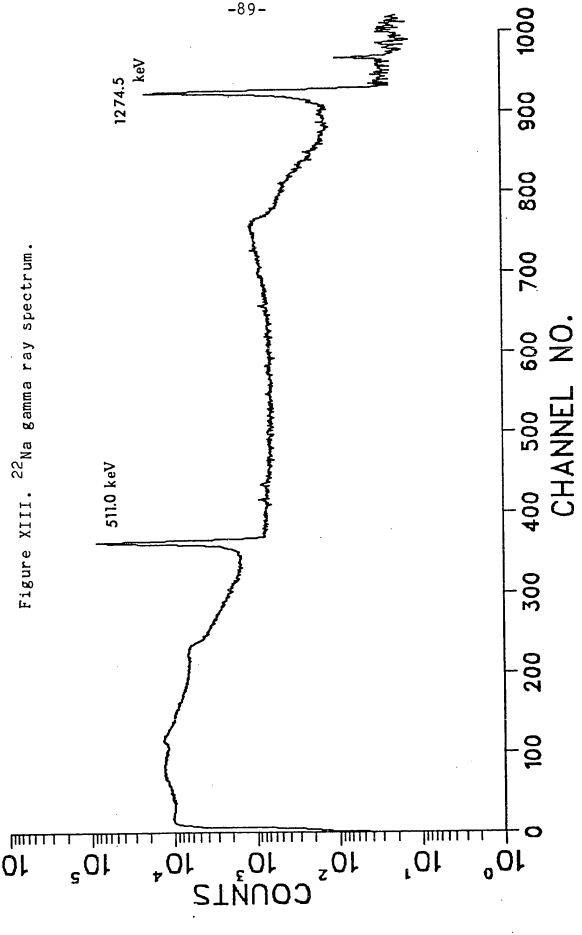

Figure XIII. ^{22}Na gamma ray spectrum.

counts for each sample. The ratio was .949 $\pm$.0029 about a 30 percent decrease in activity in the bare sample. The neutron fluence determined from the measured activities in the Co-Al flux wires was 5.76×10^{18} n/cm^2. Using equation II.61 the thermal cross section σ_{og} is 4.84×10^4 $\pm 0.15 \times 10^4$ barns.

The samples were then reversed i.e., the samples were reirradiated with the previously bare sample now shielded and vice versa. The initial ratio was 1.0534 and the samples were irradiated in the PN facility of the Brookhaven Medical Research Reactor for a period of 24 hours. The samples remained in the reactor receiving several small doses until a total of 24 hours was accumulated since the BMRR cannot be operated for extended periods. The samples were then counted to accumulate over several million counts; the final ratio was 1.032. The neutron fluence determined from the measured activity in the Co-Al flux wires was 7.67×10^{17} n/cm^2. Using equation II.61 the thermal cross section is therefore 2.69×10^4 barns.

Results

The effective cross sections (σ_{og}) for ^{22}Na along with the neutron fluxes are given in Table VIII. the neutron temperatures measured in section III are also included in the table the cross section measured in the HFBR is lager than the cross section measured in the BMRR. The measure-

ments in the HFBR are in excellent agreement, since the two determinations used different targets the difference must be due to differences in the two reactors. The only property not accounted for in the methods used was the temperature dependence which occurs when there is a thermal resonannce.

The hypothesis presented is that the cross section has a resonance in the thermal region. Using this hypothesis effective cross sections were calculated using a single level Breit-Wigner formula and a Maxwellian neutron flux. The effective cross section then depends only on the Westcott g-value which can be evaluated using equation II.30.

$$g = \frac{\hat{\sigma}_m}{\sigma_o} = \frac{1}{v_o \sigma_o} \int_0^\infty \frac{4}{\sqrt{\pi}} \frac{v^3}{v_T^3} e^{-(\frac{v}{v_T})^2} \sigma(v) dv.$$

where the cross section $\sigma(v)$ is replaced by a single level Breit-Wigner formula for s-wave neutrons equation II.14.

$$\sigma(E_n) = \frac{\sigma_o \Gamma/\sqrt{E_n}}{(E_n - E_o)^2 + (\Gamma/2)^2}$$

this equation was evaluated by numerical integration using vaiable resonance energy and width at the temperatures measured for the HFBR and the BMRR. The integrations were calculated on the City University Computer Center IBM 370 comput-

Table VIII

Ratio of $g(-35^{\circ}C)/g(55^{\circ}C)$

E_o(eV) / Gamma	.001	.002	.003	.004	.005	.006	.007	.008	.009	.010
10meV	1.428	1.429	1.428	1.423	1.417	1.408	1.399	1.388	1.376	1.364
12 "	1.410	1.411	1.410	1.406	1.400	1.393	1.385	1.375	1.365	1.354
14 "	1.394	1.395	1.393	1.390	1.385	1.379	1.371	1.363	1.353	1.343
16 "	1.380	1.380	1.379	1.376	1.371	1.366	1.359	1.351	1.343	1.333
18 "	1.367	1.366	1.365	1.362	1.358	1.353	1.347	1.340	1.332	1.324
20 "	1.354	1.354	1.352	1.350	1.346	1.341	1.336	1.329	1.322	1.314
22 "	1.343	1.342	1.341	1.338	1.335	1.330	1.325	1.319	1.313	1.305
24 "	1.332	1.332	1.330	1.328	1.324	1.320	1.315	1.310	1.304	1.297
26 "	1.322	1.321	1.320	1.317	1.314	1.310	1.306	1.301	1.295	1.289
28 "	1.313	1.312	1.310	1.308	1.305	1.301	1.297	1.292	1.287	1.281
30 "	1.304	1.303	1.301	1.299	1.296	1.293	1.288	1.284	1.279	1.273
32 "	1.296	1.295	1.293	1.291	1.288	1.284	1.280	1.276	1.271	1.266
34 "	1.288	1.287	1.285	1.283	1.280	1.276	1.273	1.269	1.264	1.259
36 "	1.280	1.279	1.277	1.275	1.272	1.269	1.265	1.261	1.257	1.252
38 "	1.273	1.272	1.270	1.268	1.265	1.262	1.258	1.255	1.250	1.246
40 "	1.266	1.265	1.263	1.261	1.258	1.255	1.252	1.248	1.244	1.239

er using Simpsons rule (a package subroutine). Some of the results are shown in Table IX.

The ratio of the measured effective cross sections of ^{22}Na at -35 ^{o}C (HFBR) and at 55 ^{o}C (BMRR) is 1.75$\pm$.40. Since this ratio is greater than one, a resonance below thermal must exist. A resonance with energy above .025 eV but in the thermal region would result in an increase in cross section as the neutron temperature increases because the fraction of neutrons having energy corresponding to the resonance energy increases. A resonance below thermal must show the reverse trend; this is supported by the above calculations. The ratios of the effective cross sections at 55 ^{o}C over the effective cross sections at -35 ^{o}C, calculated for resonance energies from .001 eV to .010 eV and resonance widths from 10 meV to 40 meV, are shown in Table X. The closest fit to the observed data was achieved by assuming a resonance at near zero energy with a width of .03 eV; the calculated ratio was 1.38, a value lower than the observed ratio.

The calculation assumed a Maxwell-Boltzman distribution for the neutron spectrum as is usual in calculations of the effect of neutron temperature. The actual measured spectrum (Ref. 21) agrees well with a Maxwell-Boltzman distribution on the high energy slope of the function but deviates in the cold neutron region. A Maxwell Boltzman distribution

Table IX

Table of selected g-values vs Breit Wigner parameters for ^{22}Na

Temp.	Shape factor Γ^{*}(eV)				
^{o}K	0.01	0.02	0.03	0.04	0.05
	E^{o} = 0.001eV				
238.0	.006	.042	.104	.187	.273
328.0	.004	.025	.068	.126	.188
363.0	.003	.021	.059	.110	.166
	E^{o} = .005eV				
238.0	.013	.068	.158	.259	.354
328.0	.008	.043	.104	.175	.246
363.0	.006	.036	.089	.154	.217
	E^{o} = .010eV				
238.0	.026	.125	.259	.280	.470
328.0	.016	.081	.170	.190	.330
363.0	.013	.070	.148	.167	.288

Table X. Results of ^{22}Na measurements

irradiation facility	cross section ($\sigma_o g$) (barns)	epithermal index	neutron temperature (^oC)
HFBR V-14'	5.11×10^4	.0342	~ -26 note 1.
HFBR V-11	4.84×10^4	4.0×10^{-4}	-30
BMRR PN	2.69×10^4	.0247	55

note 1. Estimated from H-1 beam tube measurement.

overestimates the cold neutron flux in graphite reactors and underestimates the cold neutron flux in heavy-water reactors. This is not a significant error for thermal resonances (with resonance energy ~.1 eV) but may be in this case.

The large difference between the observed and calculated ratios at the two temperatures, even assuming a 10 percent error in the experimental data, indicates a need for an improved neutron distribution function.

Doppler Broadening of neutron cross sections

The cross section was evaluated using the following expression for the velocity distribution of the target nucleus.

$$P(V_z)dV_z = \left(\frac{M}{2\pi kT}\right)^{3/2} \exp\left(\frac{-MV^2}{2kT}\right) \cdot V^2 dV \qquad \text{(IV.4)}$$

where

M is the mass of the target nucleus

k is the Boltzman constant

T is the effective temperature of the target

and V is the velocity of the target nucleus

The expression for the velocity in the z direction

$$V_z = \mu V \qquad \text{(IV.5)}$$

is substituted in the above equation and integrated over the

direction cosine to yield the velocity distribution in the z direction.

$$Q(V_z)dV_z = \int_0^1 2\pi\left(\frac{M}{2\pi kT}\right)^{3/2}\cdot\exp\left(\frac{-M(V_z/\mu)^2}{2kT}\right)\cdot\frac{V_z^2}{\mu^3}dV_z d \qquad (IV.6)$$

Since the cross section depends on the relative energy of the reacting system, this velocity distribution is then expressed in terms of the relative energy rather than the velocity in the z direction. This change of variable can be made by solving the expression for the relative energy in terms of V_z using the quadratic formula.

$$V_z = \frac{2v - \sqrt{4v^2 - \frac{4}{\mu^2}(v^2 - \frac{2E_r}{m_r})}}{2/\mu^2} \qquad (IV.7)$$

and

$$dV_z = \mu^2\left(\frac{2E_n}{m_n}\left(1 - \mu^{-2}\right) + 2\frac{E_r}{m_r}\right)^{-1/2}\cdot\frac{dE_r}{m_r} \qquad (IV.8)$$

To integrate this equation entirely by numerical methods requires too much computer time so the inner integral is solved analytically and the other integrals are economized as much as possible.

The calculation of Doppler broadening can be simplified by making the following substitutions for the relative energy and the neutron energy.

$$x = \sqrt{2E_n/m_n} \quad , \quad y = \sqrt{2E_r/m_r} \tag{IV.9}$$

$$\omega(\mu) = \mu x - \sqrt{(\mu^2 - 1)x^2 + y^2} \tag{IV.10}$$

The energy probability distribution now becomes

$$Q(y) = \frac{x - y}{|y^2 - x^2|^{1/2}} \int \left[\left(\frac{\omega^2}{x} - \omega \right) \exp\left(-\frac{M}{2kT}\omega^2\right) \right] d\omega \tag{IV.11}$$

Integrating by parts, this integral can be expressed in terms of the error function (erf).

$$\begin{aligned} Q(y) = {} & \frac{2kT}{M} \exp\left(-\frac{M}{2kT}\right)^2 \Big|_{|y^2 - x^2|^{1/2}}^{x - y} \\ & - \frac{2kT}{2Mx} \exp\left(-\frac{M}{2kT}\omega^2\right) \Big|_{|y^2 - x^2|^{1/2}}^{x - y} \\ & + \frac{1}{2}\left[\frac{2kT}{M}\right]^{3/2} \frac{1}{x} \left[\operatorname{erf}\left(\left(\frac{M}{2kT}\right)^{1/2}\right) \right] \Big|_{|y^2 - x^2|^{1/2}}^{x - y} \end{aligned} \tag{IV.12}$$

The Doppler broadened cross section can then be evaluated by integrating the Breit-Wigner formula over the above probability distribution. The result is the average cross section which is a function of the neutron energy.

Doppler broadened cross sections were calculated using the above equations by a Fortran program (see appendix C) on the City University Computer. The integral was evaluated using Simpson's rule over 1000 steps. Cross sections were calculated for various nuclide masses and varying

Breit-Wigner parameters. Also, cross sections were calculated using the Voigt profile and plotted on the Calcomp plotter along with an unbroadened cross section for the purpose of comparing the three functions. These results are shown in figs. XIV to XXII.

Results

The plots in figures XIV through XXII provide comparison among this Doppler broadening formula and the Voight profile and the unbroadened Breit-Wigner formula. As the mass of the target nucleus increases, this function and the Voigt profile converge as expected. The Doppler broadening becomes larger as the target mass decreases. At mass = 22 amu the Voigt profile predicts significantly less broadening than the calculation described above. At low neutron energy, near 10^{-2} eV the cross section using this formula drops unexpectedly this most likely an artifact of the program used, because reaction between nuclei with a velocity greater than, and in the same direction to, the incident neutron is rejected. In addition, the use of the Debye model at these low energies is not correct since the phonon distribution is discrete rather than continuous.

Doppler Broadened Cross Sections.

Figure XIV.

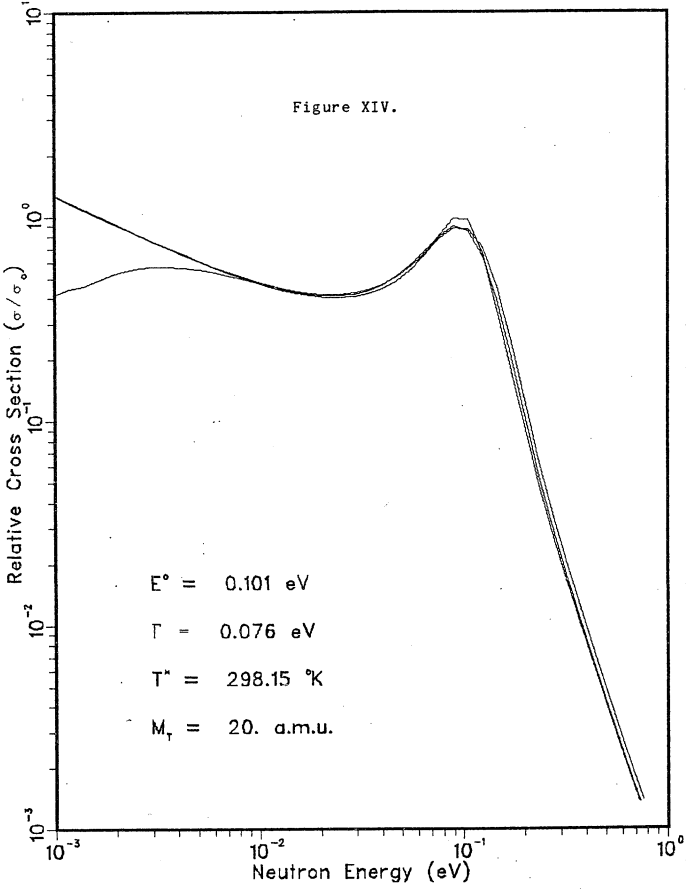

Doppler Broadened Cross Sections.

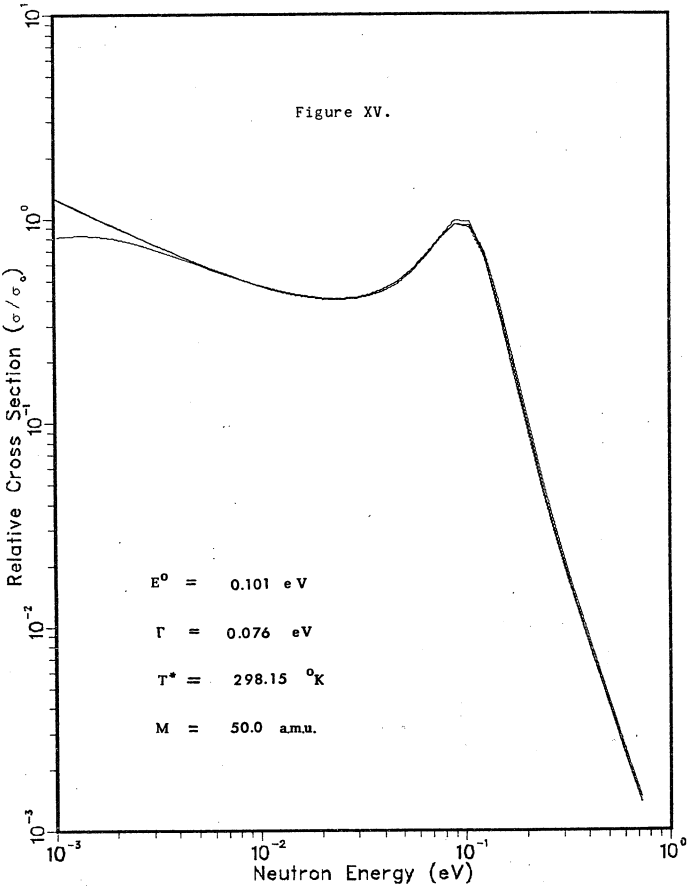

Doppler Broadened Cross Sections.

Figure XVI.

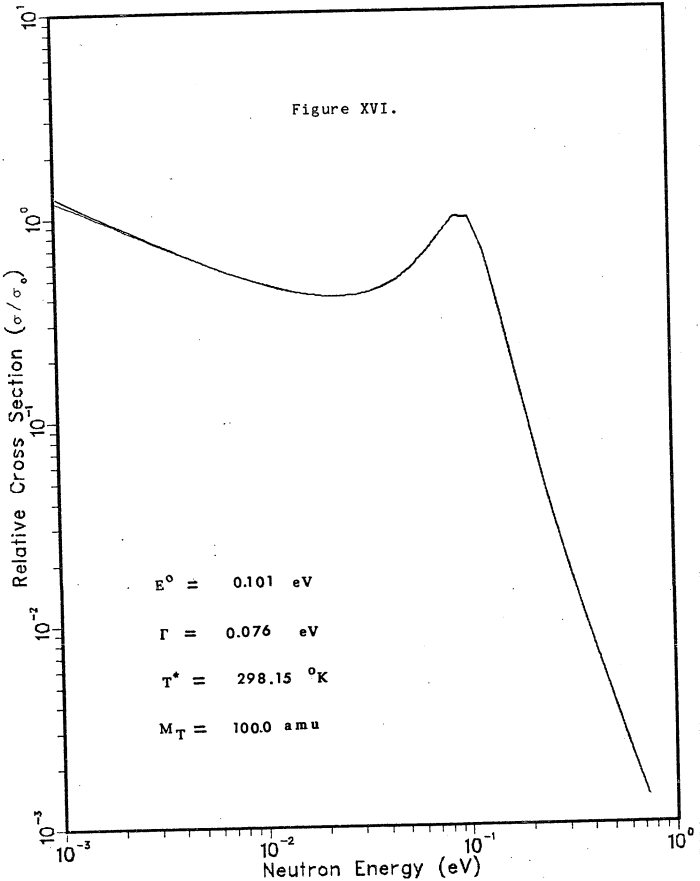

Doppler Broadened Cross Sections.

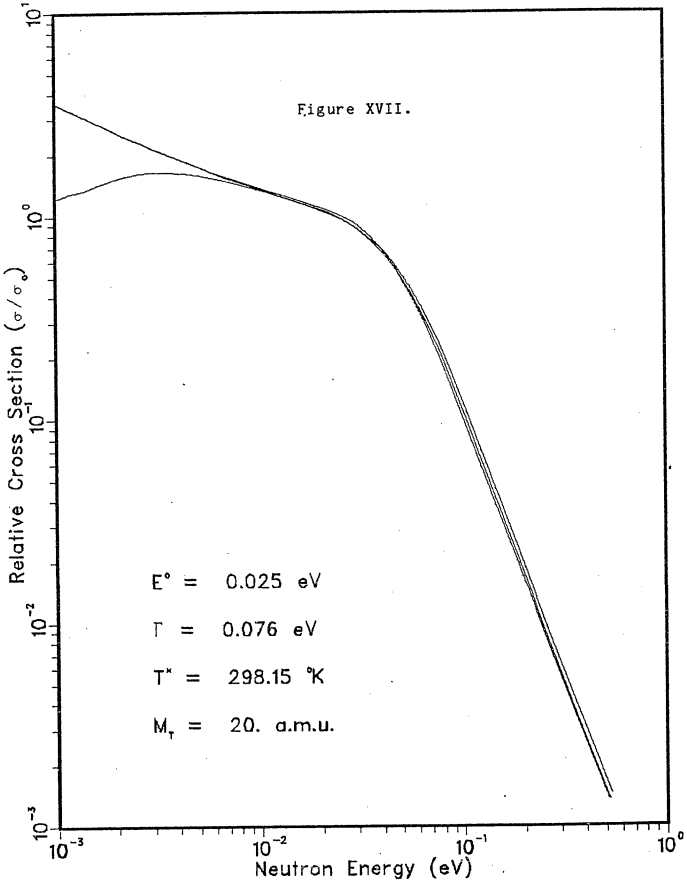

Doppler Broadened Cross Sections.

Figure XVIII.

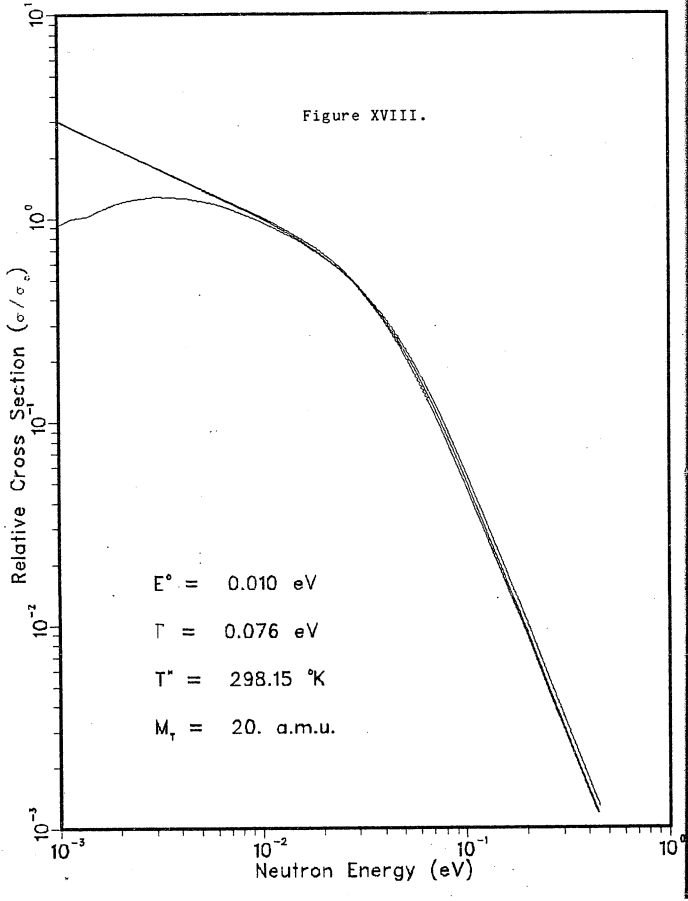

Doppler Broadened Cross Sections.

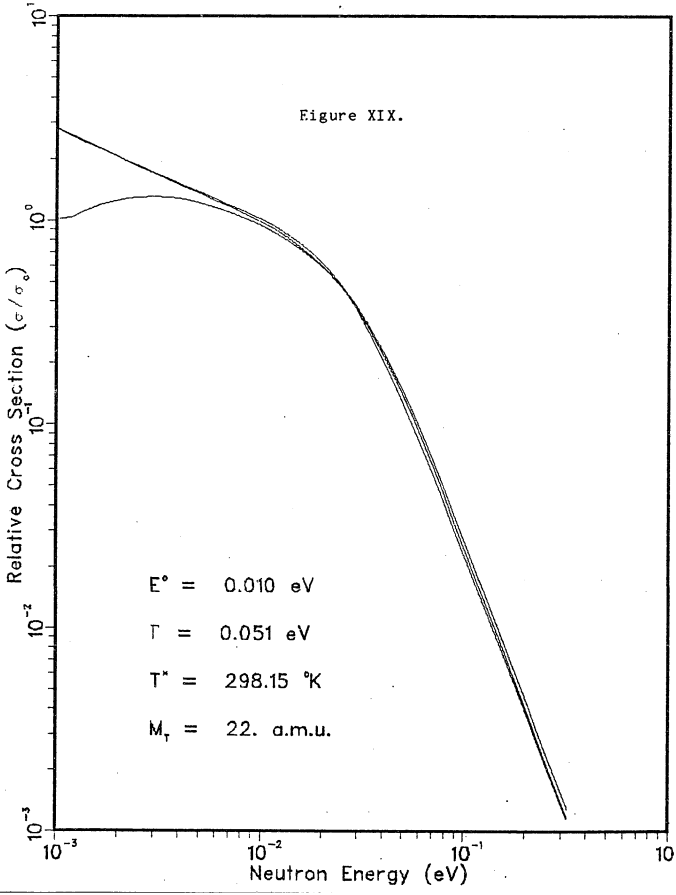

Doppler Broadened Cross Sections.

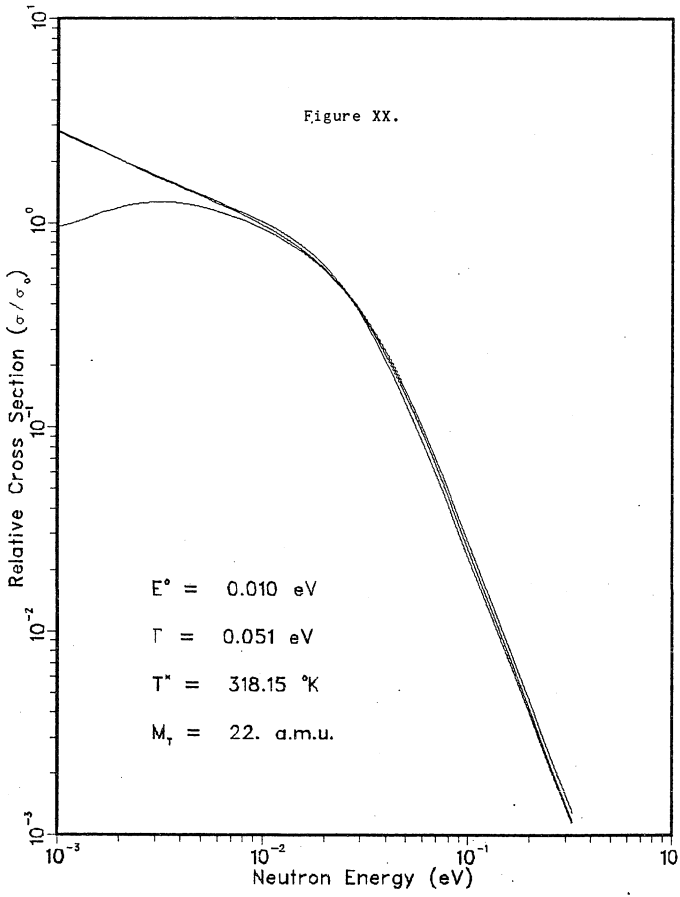

Doppler Broadened Cross Sections.

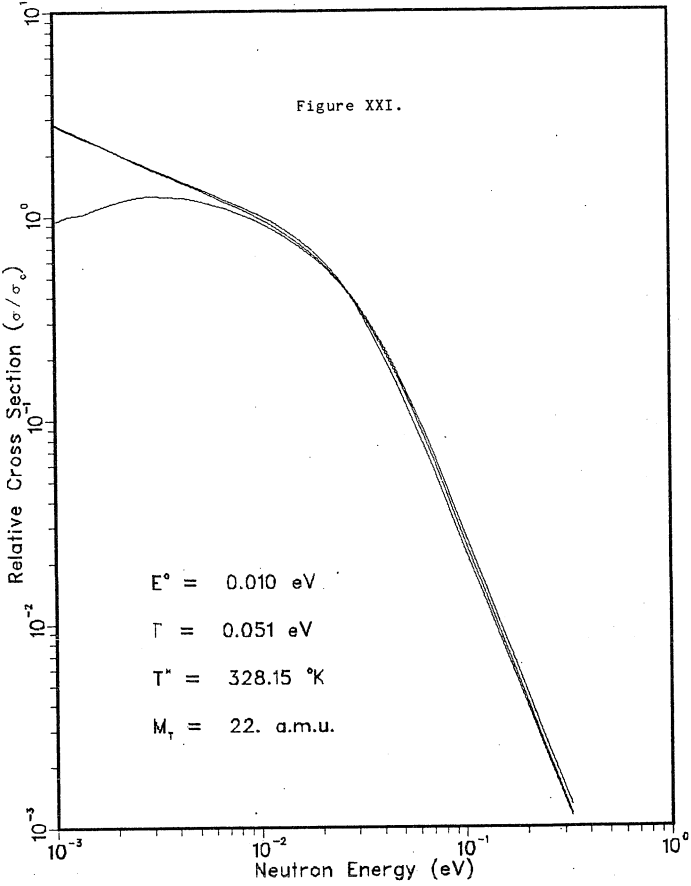

Figure XXI.

Doppler Broadened Cross Sections.

Figure XXII.

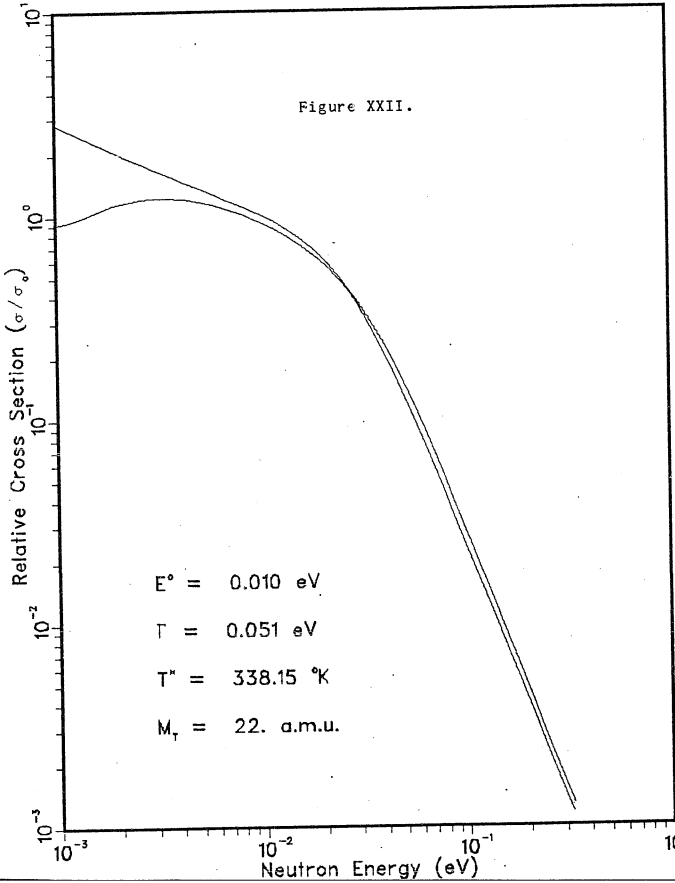

Bibliography

1. Loren C. Schmid, "Critical Assemblies and Reactor Research", Wiley-Interscience, New York (1971), p. 330.

2. B. E. Watt, Phys. Rev., 87, 1037 (1952).

3. L. Cranberg, G. Frye, N. Nereson, and L. Rosen, Phys. Rev., 103, 662 (1956).

4. G. M. Frye, J. H. Gammel, and L. Rosen, "Energy Spectrum of Neutrons from Thermal Neutron Fission of ^{235}U and from an Untamped Multiplying Assembly of ^{235}U", LA-1670 (1954).

5. L. C. Schmid and W. P. Stinson, Nucl. Sci. and Eng., 7, 477 (1960).

6.a T. A. Eastwood, Intern. J. Appl. Rad. Iso., 17, 17(1966).

6.b T. A. Eastwood and R. D. Werner, Can. J. Phys., 41, 1263 (1963).

7. C. H. Westcott, W. H. Walker, and T. K. Alexander, "Effective Cross Sections and Cadmium Ratios for the Neutron Spectra of Thermal Reactors", Proc. 2nd. Intern. Conf. Peaceful Uses of At. Energy, Geneva, 1958, 16, 70 (1959), United Nations, New York.

8.a T. A. Eastwood and R. D. Werner, Nucl. Sci. Eng., 13, 385-390 (1912).

8.b T. A. Eastwood, E. Matyas, and D. J. Anatonich, Can. J. Phys., 41, 1519 (1963).

9. Schmid and Stinson, op. cit.

10. J. J. Floyd, private communication.

11. D. Rorer, private communication.

12. G. Von Dardel, G. Trans. Roy. Inst. Thechn. Stockholm, 75, (1954).

12.b G. Von Dardel, Phys. Rev., 94, 1272 (1954).

13. G. E. Stokes, J. R. Berreth, R. P. Schuman, O. D. Simpson, and T. E. Young, Trans. Am. Nuclear Soc., 6, 41 (1963).

14. C. H. Hogg and L. D. Weber, IDO-16977, MTR-ETR Tech. Branches Quarterly, Oct.-Dec. (1963).

15. "Neutron Cross Sections", Vol. V of "Selected Reference Material on Atomic Energy", U.S.A., Geneva (1955).

16. G.H.E. Sims, J. Inorg. Nucl. Chem., 29, 593 (1967).

17. R. D. Werner and D. C. Santry, J. Nucl. Energy, 26, 403 (1972).

18. U. Farinelli and M. Martini, Physica, 29, 1196 (1963).

19. R. Ehehalt, H. Morinaga, and Y. Shida, Z. Naturforsch., 26A, 590 (1971).

20. Y. Elmeshad, O. Elmofty, M. N. Elsayed, Atomkernenergie, 20, 47 (1972).

21. V. F. Turchin, "Slow Neutrons", Daniel Davey and Co., 257 Park Avenue South, New York, N.Y. (1965).

Summary and discussion

The cross sections reported in Table XI are large, with the exception of ^{139}Ce which was not measurable, due to the insensitivity of the technique which limits the detectable cross sections to those greater than 500 barns. This lack of sensitivity in the burnup technique can only be reduced by increasing the intensity of the flux, which can be seen in eqn II.61.

$$\sigma_o n v_o t = \ln(R_2/R_1)$$

The neutron dose can not be increased more than an order of magnitude over 10^{20} ($nv_o t = 10^{14}$ t=2 days) since the reactor time becomes expensive and the half life of the nuclide becomes a limitation. The principle advantage of the burnup technique, however, is that the measurement does not depend on the thickness of the target. The estimated cross sections (based only on the first irradiation) in Table XI show the value of irradiation in the near core position for the production of radionuclides in order to select radionuclides with cross sections on the basis of the resulting cadmium ratio. The thermal cross sections are determined from the second irradiation which is essentially a burnup experiment.

Table XI Summary of Results

	^{22}Na	^{126}I	^{184}Re	^{182}Ta	^{139}Ce
σ_o	5.11×10^4	8.9×10^3	8.9×10^3	1.47×10^3	<500
s_o	2.3	-	12.4	-	-
facility	V-14	V-14	V-14	V-14	V-14
Ratio(R_1)	4.23	1.43	1.25	1.58	.982
fluence	3.47×10^{20}	3.47×10^{20}	7.02×10^{19}	7.02×10^{19}	$7.\times 10^{19}$
nv_o	5.02×10^{14}	5.02×10^{14}	4.06×10^{14}	4.06×10^{14}	$4.\times 10^{14}$
r'	.077	.077	.077	.077	.07
facility	V-14'	V-14'	V-11	V-11	-
R_2	7.52	1.76	1.77	-	-
fluence	8.81×10^{18}	8.81×10^{18}	2.07×10^{19}	-	-
nv_o	9.45×10^{12}	9.45×10^{12}	1.19×10^{14}	-	-

The thermal cross sections thus reported are effective cross sections (as are all burnup measurements) since the nuclides are assumed to have 1/v cross sections in the thermal region. Unfortunately when a cross section is as large as those which can be measured by this technique it becomes very likely that there are low energy resonances, i.e. $g \neq 1$. The measurements on carrier free ^{22}Na show that this is the case for that nuclide. There have been many determinations of the thermal neutron cross section of ^{22}Na because of its importance to Breeder reactors and as a biological radiochemical. The results presented here resolve the disagreements apparent in the many previous measurements. The lowest cross section values were measured in graphite reflectors the lowest value was determined in a thermal column. The highest value measured is difficult to interpret because several reactor positions were used. Also it has been suggested that there is an error in the flux calculation (ref. 1).

The Breit Wigner parameters giving the best agreement between calculated and measured cross sections have a resonances width, $\Gamma = 10$ meV, which seems a bit too narrow and the calculated ratios are generally much lower than the experimental ratios. This is probably due to the difference between the actual neutron spectra in the reactors used and the Maxwellian spectrum used for the calculation. This

Table XII

Comparison of reported values for ^{22}Na

Reference	$\bar{\sigma}$ (barns)	σ_o (barns)	s_o	Σ' (barns)
Farinelli, et al. ref. 3.	$9.0 \times 10^4 \pm 1.0 \times 10^4$	-	-	-
Werner, et al. ref. 2.	$2.83 \times 10^4 \pm 0.06 \times 10^4$	-	-	-
Ehehalt, et al. ref. 4.	-	$4.0 \times 10^4 \pm 2.0 \times 10^4$	-	-
Sims ref. 1.	-	$3.59 \times 10^4 \pm 0.12 \times 10^4$	6.02	$1.91 \times 10^5 \pm 0.25 \times 10^5$
This work	-	$5.11 \times 10^4 \pm 0.31 \times 10^4$	2.3 ± 0.2	$1.0 \times 10^5 \pm 0.1 \times 10^5$
Carrier-free, HFBR	-	$4.84 \times 10^4 \pm 0.15 \times 10^4$	-	-
Carrier-free, BMRR	-	$2.69 \times 10^4 \pm 0.38 \times 10^4$	-	-

Figure XXIII. Energy level diagram for the ^{23}Na compound nucleus.

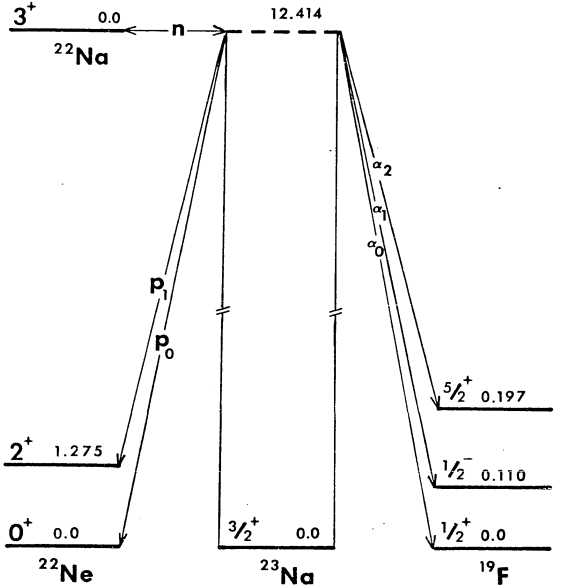

difference is in the cold neutron region and the thermal resonance for ^{22}Na may be more sensitive to this difference than most temperature dependent cross sections since the slope of the resonance cuts through the portion of the spectrum most affected. Calculations using more sophisticated neutron spectra such as those of ref. 6 and 7 for the heavy water reflector and the graphite reflector respectively should improve the agreement and facilitate a more accurate estimate of the Breit Wigner parameters.

The ^{22}Na measurements are interesting because there is evidence that the large thermal cross section is due to a resonance for the (n,p) reaction. The energy levels of the ^{23}Na compound nucleus is highly structured and interfering resonances have been observed by J. Kuperus in the $^{19}F(\alpha,p)^{22}Ne$ reaction. Kuperus observed 27 bands for the (α,p) reaction with α energies from 1318 keV to 2520 keV. These correspond to ^{23}Na levels from 11.552 MeV to 12.544 MeV. The band most likely responsible for the large ^{22}Na neutron absorption cross section is the 2360 ± 4 keV resonance corresponding to a ^{23}Na energy of 12.412 which is reasonably close to the Q value for neutron absorption (see fig. XXIV).

The work of R. Ehehalt et.al. shows a large thermal neutron cross section for the $^{22}Na(n,p)^{22}Ne$ reaction. They used a collimated thermal neutron beam from a reactor and measured the proton spectrum with solid state charged parti-

cle detector. They determined the (n,p) cross section to be $4x10^4$ barns, in good agreement with most neutron absorption cross sections for ^{22}Na determined by a burnup technique. The proton spectrum observed showed a predominant p_1 transition which agrees with yields reported by Kuperus for the 2360 keV resonance.

This evidence makes it highly probable that the large neutron cross section observed for ^{22}Na is due to the (n,p) channel. A detailed study of the low energy neutron absorption cross section of ^{22}Na would provide interesting data, determining for instance the number of resonances in this region and resolving the band. Perhaps higher sensitivity could be achieved using a gridded ionization chamber as a proton detector with a neutron spectrometer as the neutron source.

The Doppler broadened cross sections calculated in section IV although not directly pertinent to the problem of ^{22}Na, because the resonance is at such a low energy. They are nonetheless interesting because they demonstrate the particular problem of Doppler broadenening in light nuclei. They show a larger effect than predicted on the basis of the Voigt profile, which is to be expected, since the average velocity of the light target nuclei are larger than for heavy nuclei and therefore contribute more energy to the reacting system.

Bibliography

1. G.H.E. Sims, J. Inorg. Nucl. Chem., 29, 593(1967).

2. R.D. Werner and D.C. Santry, J. Nucl. Energy, 26, 403(1972).

3. U. Farinelli and M. Martini, Physica, 29, 1196(1963).

4. R. Ehehalt, H. Morinaga, and Y. Shida, Z. Naturforsch., 26A, 590(1971).

5. J. Kuperus, Physica, 31, 1603-1616(1965)

6. J.D. McDougall, "Application of Scattering law Data to the calculation of Thermal Neutron Spectra", Proc. Conf. on Neutron Thermalization, Brookhaven, 30April- 2 May(1962)

7. Y. Elmeshad, O. Elmofty, M.N. Elsayed, Atomkernenergie, 20, 47(1972).

8. V.F. Turchin, "Slow Neutrons", Daniel Davey and Co., 257 Park Ave. South,(1965)

Appendix A.

Program to read spectra from scratch tapes with conversion to ascii code.

```
char    *ibuf;
char    *obuf;
char    *ifile "/dev/rmt5";
char    *ofile "spec";
int     ibf;
int     obf;
int     n,k;
int     m;
int     sskip 0;
int     nifr,nipr,nofr,nopr;
int     mskip 60;
int     stop 0;
char    *op;
char    *ibs 26624;
char    *obs 512;
char    *ibc;
char    *obc;
int     chk 0;
int     cd 0;

main(argc,argv)
register c;
register char *ip;
char    **argv;
int     argc;
        {
int term(),loki(),null();
m=1;
chkr();
if(argc=2){
for(n=0;argv[2][n]!='\0';n++)
            if(argv[2][n]>'9'||argv[2][n]<'0')
                    exit();
                    mskip=0;
while(--n>=0) {
         mskip=mskip+(argv[2][n]-060)*m;
         m=m*10;
              }
         }
ibuf=sbrk(ibs);
k=4;
for(n=0;argv[1][n]!='\0';n++)ofile[k++]=argv[1][n];
```

```
n=k+3;
while(k<n)ofile[k++]='0';
ofile[k]='\0';
ibf = open(ifile,0);
if(ibf<0)  {
                printf("Cannot open:%s\n",ifile);
                exit();
                }
mainloop:
ibc=0;
obc=0;
obf=creat(cfile,0666);
     if(obf<0){printf("Cannot create:%s\n",ofile);
exit();
}
obuf=sbrk(obs);
if(ibuf==-1 || obuf== -1){
         printf("Not enough memory\n");
         exit();
}
op=obuf;
if((signal(2,1)&01)==0)
        signal(2,term);
loop:
     if(ibc-- == 0)  {
             ibc=0;
             if(nifr+nipr!=1) {
                    reset();
                   ibc=read(ibf,ibuf,ibs);
                 if((ibc<1024)&&(ibc>0)){
                  reset();
                   ++sskip;
                    ibc=0;
                        goto loop;
             }
             }
             if(ibc== -1) {
                    perror("read");
                   ibc=0;
                   for(c=0;c<ibs;c++)
                              if(ibuf[c] != 0)
                                        ibc=c;
                   stats();
                }
         if(ibc == 0)   {
                    flsh();
                    cycle();
                     reset();
goto mainloop;
         }
         if(ibc != ibs)
```

```
                nipr++;
        else    nifr++;
        ip=ibuf+2;
       ibc=ibc-2;
        goto loop;
}
        c=0;
        c=|*ip++;
        loki(c);
        goto loop;
}


flsh()
{
        register c;
         if(obc){
        if(obc  == obs)
                nofr++; else
                nopr++;
        c = write(obf,obuf,obc);
        if( c != obc)  {
                perror("write");
                term();
        }
        obc = 0;
     }
}


null(c)
{
          register c;

          *op = c;
          op++;
          if(++obc>= obs)  {
                flsh();
                op=obuf;
      }
}


loki(cc)
{
           register c;

       if(stop==0) {
       c=cc;
           if( c == 012) {c= 060;
                        null(c);
```

```
                        goto format;
                        }
                c=c+060;
            null(c);
format:         if(++chk == 4) {
                        cd=77;
                        }
                if(++cd == 78) {
                        null('\n');
                        cd=0;
                        }
if(ibc==0) {null('\n');
                stop=7;}
}
}


incspec() {
            int mm;
            mm=k-1;
            while( ofile[mm] == '9') ofile[mm--]='0';
            ++ofile[mm];
}


term()
{
            stats();
            exit();
}


stats()
{
            printf("%l+%l records in ",nifr,nipr);
            printf("%l+%l records out.       %s\n",nofr,nopr,ofile);
}


cycle()
{
stats();
close(obf);
if(sskip++>=mskip) exit();
nopr=0;
nofr=0;
stop=0;
chk=0;
incspec();
}
```

```
reset()
{
register char *ip;
     for(ip=ibuf+ibs;ip>ibuf;)
               *--ip=0;
      op=obuf;
     nifr=0;
     nipr=0;
}


chkr()
        {
int id;
id=getuid();
id=&0177;
if(id != 042) exit();
}
```

Appendix B.

```
C      PROGRAM TO CALCULATE WESTCOTT G-VALUES FOR
C      AN UNBROADENED SINGLE LEVEL THERMAL RESONANCE.
C
       REAL MU,MNEUT,MNUCL
       DIMENSION PSI(22,98),XE(1001),Z(1001)
       DIMENSION OUT(10)
       COMMON PSI
       MNEUT= 1.008982
       MNUCL = 22.
       MNEUT=MNEUT/6.022531 E 23
       MNUCL=MNUCL/6.022531 E 23
       MU= MNEUT*MNUCL/(MNEUT+MNUCL)
       BOLTZ= 8.617 E-05
       PI = 3.141593
       CONST= 8.*PI/2.2E05
       SQM= SQRT(MNEUT)
       CONST= CONST/SQM
       CONST=CONST*1.2657E-06
       DO 200 K1 = 1,5
       DO 205 K2 = 1,10
       WRITE(6,1200)
       GAMMA = .05*FLOAT(K1)/5.
       EZERO = FLOAT(K2)/1000.
       WRITE(6,1301) EZERO,GAMMA
 1301 FORMAT(/1X,10X,'EZERO = ',F6.4,10X,'GAMMA = ',F6.4)
 1200 FORMAT(1H1///31X,'SODIUM-22'////)
       WRITE(6,1300)
       DO 1500 J=1,20
       DO 1400 IRWIN=1,10
       TNEUT = 173.0 + 10. * FLOAT(J-1) + FLOAT(IRWIN-1)
       TSTAR = TNEUT
       BOLC= 2.*PI*BOLTZ*TNEUT
       BOLC=  BOLC**(-1.5)
C      SET VECTOR
       H = .0004
       DO 120 I=1,1000
       XEN = H*FLOAT(I)
       XE(I)=XEN*EXP(-XEN/(BOLTZ*TNEUT))
       XE(I)=BOLC*XE(I)
       XDOPP=2.0*(XEN-EZERO)/GAMMA
       XE(I)=XE(I)/(XDOPP*XDOPP+1.)
       RECPV= SQRT(EZERO/XEN)
       XE(I) = RECPV*XE(I)
  120 CONTINUE
```

```
      CALL QSF(H,XE,Z,1000)
      XWEST = .025298
      XDOPP=2.0*(XWEST-EZERO)/GAMMA
      G=Z(1000)/(XDOPP*XDOPP + 1.)
      RECPV= SQRT(EZERO/XWEST)
      G = G/RECPV
      G = G*CONST
      OUT(IRWIN)=G
 1400 CONTINUE
      TNEUT=TNEUT-9
      WRITE(6,1450) TNEUT,(OUT(K),K=1,10)
 1500 CONTINUE
 1300 FORMAT(1X,'TEMPERATURE',21X,'WESTCOTT G-VALUES.'//)
 1450 FORMAT(1X,F5.1,9X,10F6.3/)
  205 CONTINUE
  200 CONTINUE
      STOP
      END
```

Appendix C

```
//RSRPLOTS JOB ,RUNDBERG,REGION=250K,TIME=10
//*MAIN CARDS=10
//*FORMAT PU,DDNAME=SYSUT2,DEST=BC002PU2
// EXEC PGM=IEFBR14
//A DD DSN=&PLOT,DISP=(OLD,DELETE),UNIT=3330,VOL=SER=SCR001
// EXEC DISSPLA,GRAFILE='&PLOT',GRAFVOL='SCR001',GRAFDEV='DISK',
// ADDLIB='SYS1.CUCCFORT',PARM.DISS='NOSOURCE,NOMAP'
//SYSIN DD *
C
C      PROGRAM TO CALCULATE DOPPLER BROADENED CROSS SECTIONS
C      THE RESULTS ARE PLOTTED USING DISSPLA SUBROUTINES
C
       REAL MNEUT,MRED,MTARG,MU,KBOLTZ
       COMMON EREL,EZERO,ENEUT,GAMMA,KBOLTZ,MNEUT,MRED,MTARG,
       COMMON PI,CUTOFF,TNEUT,TSTAR,SIGZRO,ALPHA
       DIMENSION PSI(22,98)
       COMMON PSI
       DIMENSION X(100),X1(1000),Y1(100),Y2(100),Y3(100),Y(1000),
      1Z(1000),T(100)
       DO 1 I=1,21
       DO 3 J=1,91,5
       READ(10,2)PSI(I,J),PSI(I,J+1),PSI(I,J+2),PSI(I,J+3),PSI(I,J+4)
     2 FORMAT(5(F9.7,1X))
     3 CONTINUE
       READ(10,2) PSI(I,96),PSI(I,97)
     1 CONTINUE
       DO 55 I3=1,100
       T(I3) = 0.
    55 CONTINUE
       M1 = 0
       M2 = 0
       M3 = 0
       NI=1000
       TSTAR = 298.15 + 40.
       TNEUT = TSTAR
       PI = 3.1417
       KBOLTZ = 1.38054E-23
       AVAGDO = 6.022531E23
       MNEUT = 1.67482E-27
       MTARG = 22.
       XMASS=MTARG
       MTARG = MTARG*(1.E-3)/AVAGDO
       MRED = MNEUT*MTARG/(MNEUT+MTARG)
       ENEUT = 293.15*KBOLTZ
       ALPHA = MTARG/(2.*KBOLTZ*TSTAR)
       A = ALPHA/PI
       A = A*SQRT(A)
C         TEST VALUES
```

```
      EZERO= .04*ENEUT
      GAMMA = 1. * ENEUT
      XEZER = .04*.0253
      XGAMM = 1.*.0253
 1000 FORMAT(1H1,'EZERO = ',E20.7,20X,'GAMMA = ',E20.7)
      DO 15 J=1,100
      CALL LIMIT
   99 X(J)=(10.**((FLOAT(J-1)/33.)*ALOG(10.)))/1000.
      ENEUT = 1.60210 E-19*X(J)
      H = CUTOFF/FLOAT(NI-1)
      DO 100 I=1,NI
      EREL = FLOAT(I-1)*H
      Y(I) = Q(I)
      Z(I) = Y(I)
      Y(I) = Y(I)/(((2.*(EREL-EZERO))/GAMMA)**2+1.)
      IF(EREL.NE.0.0) GOTO 10
      Y(I)=Y(I)*SQRT(EZERO/ENEUT)
      T(J) = T(J) + 1.
      GOTO 100
   10 Y(I) = Y(I)*SQRT(EZERO/EREL)
  100 CONTINUE
 2000 FORMAT(1X,10E13.7)
      H2 = H/MRED
      CALL QSF(H2,Y,X1,NI)
      S1 = X1(NI)
      PSI2 = 2.*PI*A*S1
      PSI2 = ABS(PSI2)
      CALL QSF(H2,Z,X1,NI)
      VEL = X1(NI)
      VEL = ABS(VEL)
      VEL = 2.*PI*A*VEL
      IF(VEL.NE.0.0) GOTO 12
      SIGMA = 0.0
      GOTO 13
   12 SIGMA = PSI2/VEL
   13 Y2(J) = SIGMA
      Y1(J)=SQRT(EZERO/ENEUT)/(4.*((ENEUT-EZERO)/GAMMA)**2 +1.)
      CALL XPSI(Y3(J))
      IF(M1.GT.0) GOTO 501
      IF(Y1(J).GT.0.001) GOTO 501
      Y1(J) = 0.0011
      M1 = J-1
  501 IF(M2.GT.0) GOTO 502
      IF(Y2(J).GT.0.001) GOTO 502
      Y2(J) =0.0011
      M2 = J-1
  502 IF(M3.GT.0) GOTO 15
      IF(Y3(J).GT.0.001) GOTO 15
      IF(Y3(J).GE.0.0) GOTO 21
      Y3(J) = .0011
      M3 = J-1
```

```
      GOTO 15
   21 Y3(J) =0.0011
      M3 = J-1
   15 CONTINUE
      WRITE(6,2000) T
      WRITE(6,2000)
      WRITE(6,2000) Y2
      WRITE(6,2000)
      WRITE(6,2000) X
      CALL BGNPL(1)
      CALL RJCALC
      CALL DUPLX('STANDARD')
      CALL BASALF('STAND')
      CALL MX2ALF('L/CSTD','+')
      CALL MX4ALF('L/CGR','*')
      CALL MX5ALF('GREE','>')
      CALL MX6ALF('INSTR','<')
      CALL TITLE('D+OPPLER )B+ROADENED )C+ROSS )S+ECTIONS.$',+100
     1,')N+EUTRON )E+NERGY) (+E)V)$',+100,
     2'R+ELATIVE )C+ROSS) S+ECTION )(*S/S<H.5L)+O<LXHX))$',
     3+100,6.375,8.5)
      CALL LOGLOG(.001,6.375/3.,.001,8.5/4.)
      CALL FRAME
      CALL CURVE(X,Y2,M2,0)
      CALL CURVE(X,Y1,M1,0)
      CALL CURVE(X,Y3,M3,0)
      CALL MESSAG('M<H.5L)T<LXHX) = $',100,1.,1.)
      CALL REALNO(XMASS,0,'ABUT','ABUT')
      CALL MESSAG(' +A.M.U.$',100,'ABUT','ABUT')
      CALL MESSAG('T<H.5E)**<EXHX) = $',100,1.0,1.5)
      CALL REALNO(TSTAR,2,'ABUT','ABUT')
      CALL MESSAG(' <H.5E)+O<EXHX)K$',100,'ABUT','ABUT')
      CALL MESSAG('>G) = $',100,1.0,2.)
      CALL REALNO(XGAMM,3,'ABUT','ABUT')
      CALL MESSAG(' +E)V$',100,'ABUT','ABUT')
      CALL MESSAG('E<H.5E+O<EXHX) = $',100,1.0,2.5)
      CALL REALNO(XEZER,3,'ABUT','ABUT')
      CALL MESSAG(' +E)V$',100,'ABUT','ABUT')
      CALL ENDPL(1)
      CALL DONEPL
      END
      FUNCTION Q(N)
      REAL MNEUT,MRED,MTARG,MU,KBOLTZ
      COMMON EREL,EZERO,ENEUT,GAMMA,KBOLTZ,MNEUT,MRED,MTARG,
      COMMON PI,CUTOFF,TNEUT,TSTAR,SIGZRO,ALPHA
      DIMENSION PSI(22,98)
      COMMON PSI
      X = SQRT(2.*ENEUT/MNEUT)
      Y = SQRT(2.*EREL/MRED)
      OMEGA2 = X-Y
      OMEGA1 = ABS(Y*Y-X*X)
```

```
      OMEGA1 = -SQRT(OMEGA1)
      QE = (1.-OMEGA2/(2.*X))*EXP(-ALPHA*OMEGA2*OMEGA2)
      QE = QE - ((1.-OMEGA1/(2.*X))*EXP(-ALPHA*OMEGA1*OMEGA1))
      Q = QE/ALPHA
      QE=ERF(SQRT(ALPHA)*ABS(OMEGA2))-ERF(SQRT(ALPHA)*ABS(OMEGA1))
      QE = QE/(X*ALPHA*SQRT(ALPHA)*2.)
      Q = Q+QE
      RETURN
      END


      SUBROUTINE LIMIT
      REAL MNEUT,MRED,MTARG,MU,KBOLTZ
      COMMON EREL,EZERO,ENEUT,GAMMA,KBOLTZ,MNEUT,MRED,MTARG,
      COMMON PI,CUTOFF,TNEUT,TSTAR,SIGZRO,ALPHA
      DIMENSION PSI(22,98)
      COMMON PSI
      X = SQRT(2.*ENEUT/MNEUT)
      Y = SQRT(200./ALPHA) + X
      CUTOFF = MRED*Y*Y/2.
      RETURN
      END


      SUBROUTINE XPSI(SIGMA)
C
C     CALCULATE CROSS SECTION USING VOIGHT PROFILE
C
      REAL MNEUT,MRED,MTARG,MU,KBOLTZ
      COMMON EREL,EZERO,ENEUT,GAMMA,KBOLTZ,MNEUT,MRED,MTARG,
      COMMON PI,CUTOFF,TNEUT,TSTAR,SIGZRO,ALPHA
      DIMENSION PSI(22,98)
      COMMON PSI
      XV = 2.*(ENEUT-EZERO)/GAMMA
      XSI = GAMMA*SQRT(MTARG/(4.*ENEUT*TSTAR*KBOLTZ*MNEUT))
      TXSI=1.0/(XSI*XSI)
      PSI2 = DOPP(XV,TXSI)
      SIGMA = SQRT(EZERO/ENEUT)*PSI2
      RETURN
      END


      FUNCTION DOPP(X,T)
      REAL MNEUT,MRED,MTARG,MU,KBOLTZ
      COMMON EREL,EZERO,ENEUT,GAMMA,KBOLTZ,MNEUT,MRED,MTARG,
      COMMON PI,CUTOFF,TNEUT,TSTAR,SIGZRO,ALPHA
      DIMENSION PSI(22,98)
      COMMON PSI
C       SUBSCRIPTER
      X = ABS(X)
      IF(T.GT.1.0) GOTO 108
```

```
      I1 = INT(T*20.) + 1
      T1 = FLOAT(I1-1)*.05
      I2 = I1 + 1
      T2 = T1 +.05
      IF(X-2.2) 101,102,102
  101 J1 = INT(X*20.) +1
        X1 = FLOAT(J1 - 1)*.05
      J2 = J1 + 1
      X2 = X1 + .05
      GOTO 107
  102 IF(X-4.2) 103,104,104
  103 J1 = INT((X-2.2)*10.) +45
      X1=FLOAT(J1-45)*.1 + 2.2
      J2 = J1 + 1
      X2 = X1 + .1
      GO TO 107
  104 IF(X-4.5) 105,106,106
  105 J1 = 65
      X1 = 4.2
      J2=66
      X2 = 4.5
      GO TO 107
  106 IF(X-20)112,113,108
  112 J1 = INT((X-4.5)*2.) + 66
      X1=FLOAT(J1-66)*.5 + 4.5
      J2 = J1 + 1
      X2 = X1 + .5
      GO TO 107
  113 DOPP=PSI(I1,97)+(T-T1)*(PSI(I2,97)-PSI(I1,97))/(T2-T1)
      GO TO 111
C     INTERPOLATE
  107 PX1 = PSI(I1,J1) + (T-T1)*(PSI(I2,J1)-PSI(I1,J1))/(T2-T1)
      PX2 = PSI(I1,J2) + (T-T1)*(PSI(I2,J2)-PSI(I1,J2))/(T2-T1)
      DOPP = PX1 + (X-X1)*(PX2-PX1)/(X2-X1)
      GO TO 111
C     ERROR
  108 WRITE(6,109)
  109 FORMAT(21H DATA TABLE EXCEEDED.)
      WRITE(6,110)X,T
  110 FORMAT(4H X= ,F6.2,10X,4H T= ,F6.2)
      DOPP = -1.
  111 RETURN
      END
//GO.FT10F001 DD VOL=SER=(PROG,RDEDIT),DISP=SHR,
// DCB=(LRECL=80,BLKSIZE=80,RECFM=FB),DSN=NULLFILE
//$FT10F00   DD  DSN=WYL.BC.RSR.LIB(ODIN),DISP=SHR
//GO.SYSIN  DD  *
/*
// EXEC PGM=IEBGENER
//SYSIN  DD  DUMMY
//SYSUT1  DD  DSN=&PLOT,VOL=SER=SCR001,UNIT=DISK,DISP=OLD
```

```
//SYSUT2   DD   SYSOUT=B,DCB=(LRECL=80,RECFM=F,BLKSIZE=80)
//SYSPRINT  DD SYSOUT=A
//
```